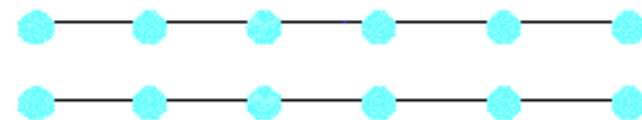


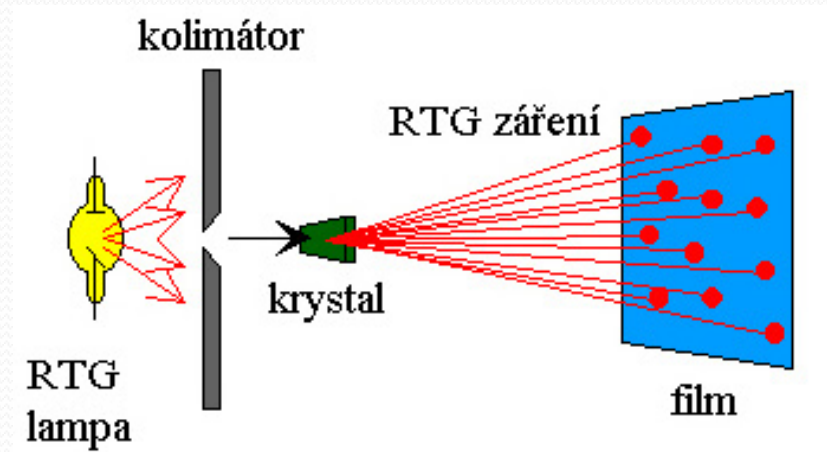
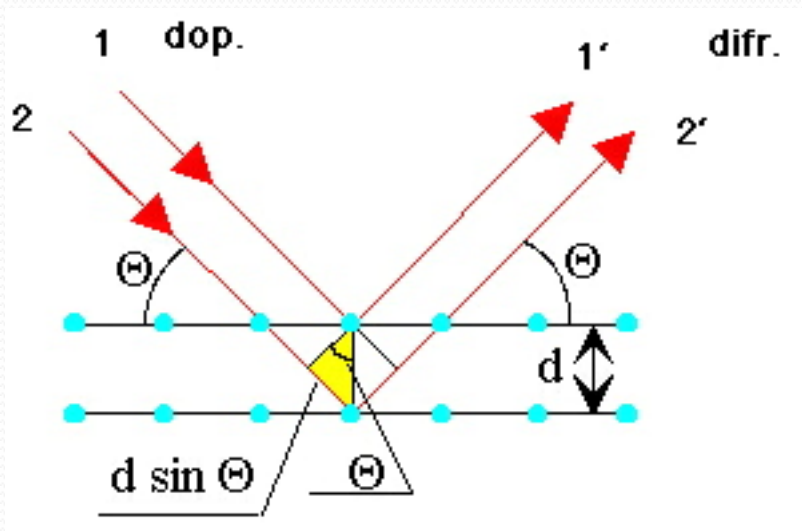
Rentgenová difraktometrie

- **Princip difraktometrie –**

- ohyb (difrakce) paprsků a jejich interference



$$2d \sin \Theta = n \lambda \quad n=1,2,3\dots$$



Rentgenová difraktometrie



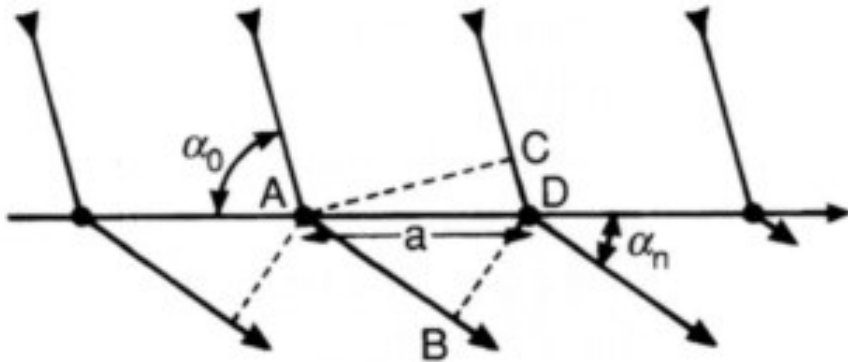
- Historické poznámky
 - Max von Laue (9. října 1879, Pfaffendorf – 24. dubna 1960, Berlín) – laueogram
 - 1912 - RTG difrakce na krystalech
 - 1914 – Nobelova cena za fyziku
 - Model difrakčního procesu – RTG záření rozkmitá elektronové obaly atomů a ty se stanou zdrojem sekundárního koherentního RTG záření, interference sekundárního záření způsobí, že v některých směrech dojde k zesílení intenzity, v jiných k zeslabení
 - difrakční obrazec
 - Laueovy rovnice

$$\mathbf{a}_1 \cdot (\mathbf{s} - \mathbf{s}_0) = a_1 (\cos \alpha_1 - \cos \alpha_{10}) = k_1 \lambda$$

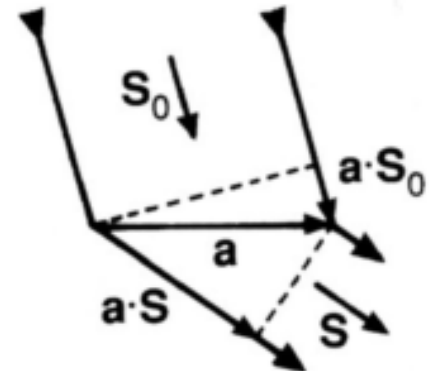
$$\mathbf{a}_2 \cdot (\mathbf{s} - \mathbf{s}_0) = a_2 (\cos \alpha_2 - \cos \alpha_{20}) = k_2 \lambda$$

$$\mathbf{a}_3 \cdot (\mathbf{s} - \mathbf{s}_0) = a_3 (\cos \alpha_3 - \cos \alpha_{30}) = k_3 \lambda$$

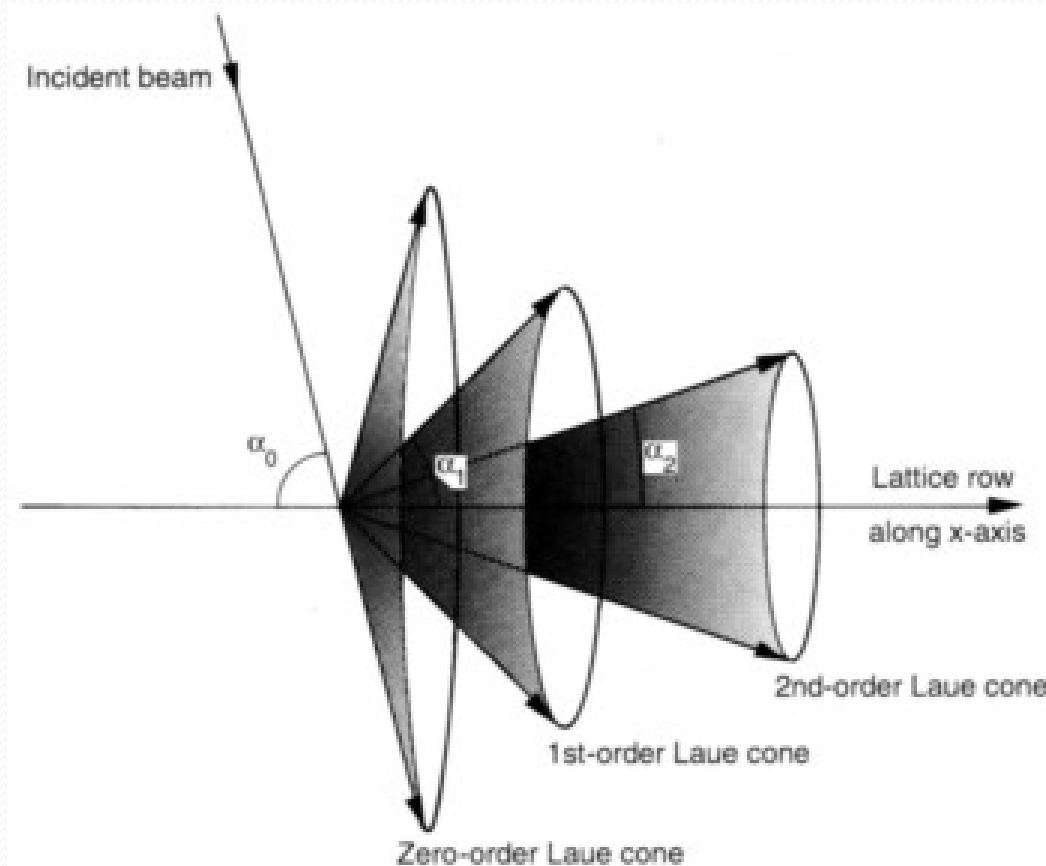
Rentgenová difraktometrie



- řada atomů podél osy x s periodickou vzdáleností a
- $(AB - CD) = a (\cos \alpha_n - \cos \alpha_0) = n \lambda$
- vektorově $\mathbf{a} (\mathbf{s} - \mathbf{s}_0) = a (\cos \alpha_n - \cos \alpha_0) = n \lambda$



Rentgenová difraktometrie



- vektorově $\mathbf{a} (\mathbf{s} - \mathbf{s}_0) = a (\cos \alpha_n - \cos \alpha_0) = n \lambda$
 - podle hodnoty n (řádu difrakce) – jednotlivé (Laueho) kužely

Rentgenová difraktometrie



- vektorově $\mathbf{a} (\mathbf{s} - \mathbf{s}_0) = a (\cos \alpha_n - \cos \alpha_0) = n \lambda$
 - obdobné vyjádření pro periodicitu atomů podél další os – celkově tedy soustava rovnic

$$\mathbf{a}_1 \cdot (\mathbf{s} - \mathbf{s}_0) = a_1 (\cos \alpha_1 - \cos \alpha_{10}) = k_1 \lambda$$

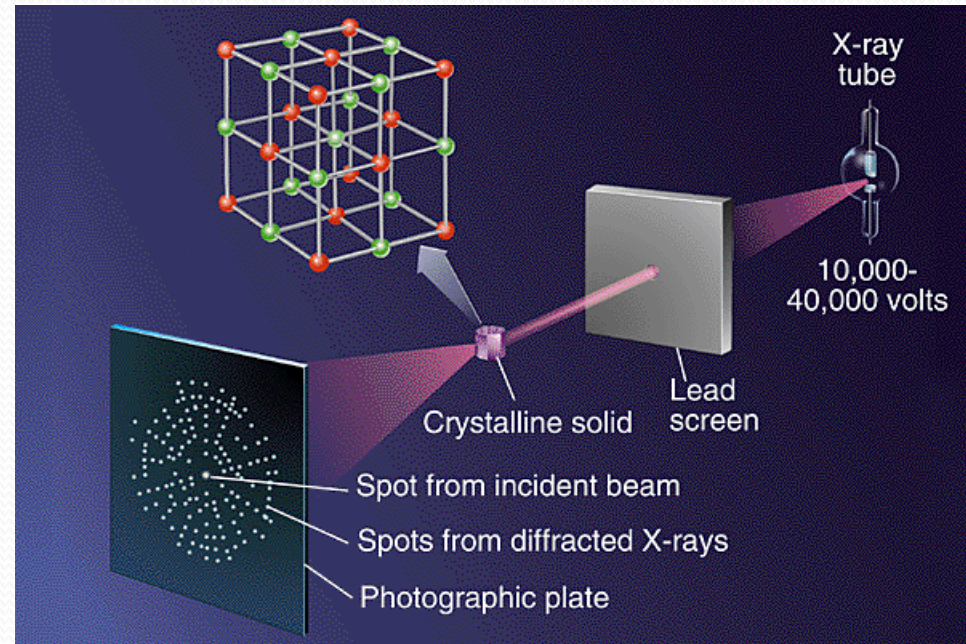
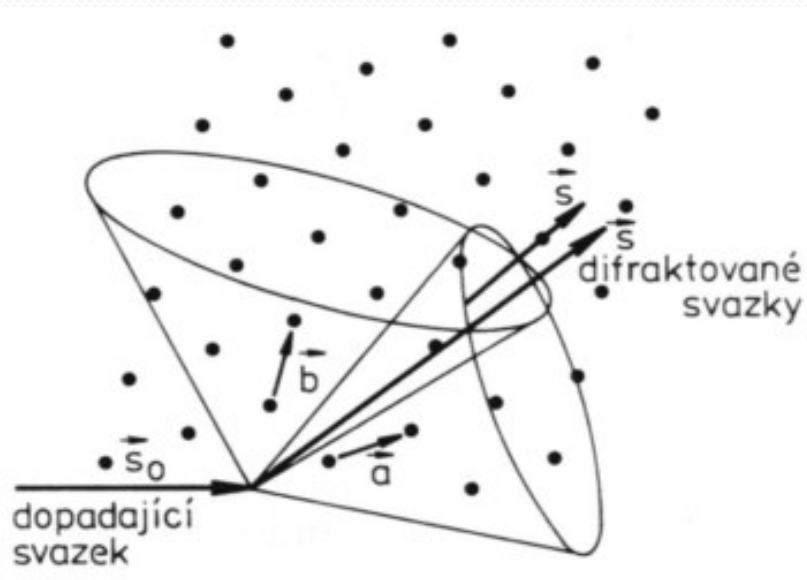
$$\mathbf{a}_2 \cdot (\mathbf{s} - \mathbf{s}_0) = a_2 (\cos \alpha_2 - \cos \alpha_{20}) = k_2 \lambda$$

$$\mathbf{a}_3 \cdot (\mathbf{s} - \mathbf{s}_0) = a_3 (\cos \alpha_3 - \cos \alpha_{30}) = k_3 \lambda$$

- Parametry k_1 , k_2 a k_3 značeny též h , k , l
- Nutno splnit všechny tři rovnice zároveň

Souvislost
s Millerovými indexy
pro kubickou
symetrii

Rentgenová difraktometrie



$$\mathbf{a}_1 \cdot (\mathbf{s} - \mathbf{s}_0) = a_1 (\cos \alpha_1 - \cos \alpha_{10}) = k_1 \lambda$$

$$\mathbf{a}_2 \cdot (\mathbf{s} - \mathbf{s}_0) = a_2 (\cos \alpha_2 - \cos \alpha_{20}) = k_2 \lambda$$

$$\mathbf{a}_3 \cdot (\mathbf{s} - \mathbf{s}_0) = a_3 (\cos \alpha_3 - \cos \alpha_{30}) = k_3 \lambda$$

Úseky a_1 , a_2 a a_3 značeny též a , b , c

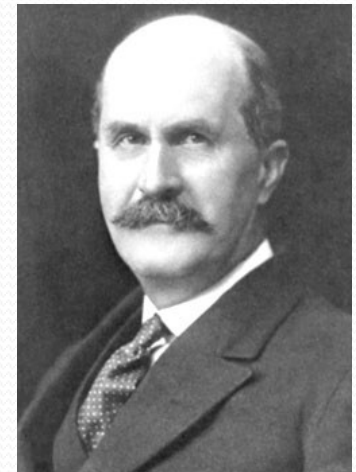
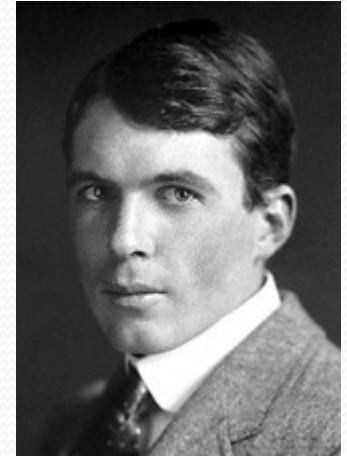
Rentgenová difraktometrie

- Interakce RTG záření s elektrony atomů
- Intenzita „rozptýleného“ záření – počet elektronů v atomu (u elektroneutrálního atomu odpovídá atomovému číslu) – atomový faktor f
- Intenzita interferenčních maxim - populace atomů v difrakčních rovinách – Millerovy indexy
- strukturní faktor $F(h,k,l)$ – h, k, l – Millerovy indexy
 - u_n, v_n, w_n - souřadnice n -tého atomu

$$F(h, k, l) = \sum_n f_n \exp[-2\pi i(hu_n + kv_n + lw_n)]$$

Rentgenová difraktometrie

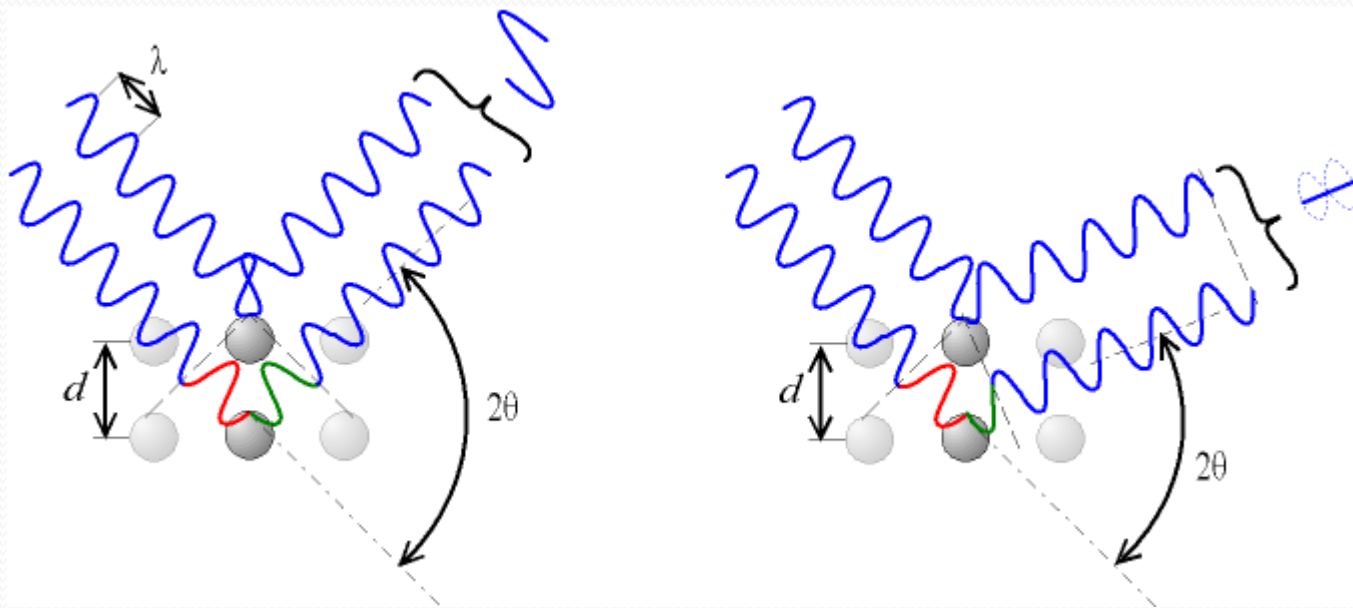
- Historické poznámky
 - William Lawrence Bragg (31.března 1890 – 1. července 1971)
 - Matematický popis fyzikálního problému
 - Formuloval Braggovu rovnici
 - William Henry Bragg (2. července 1862 – 10. března 1942)
 - Experimentátor, konstruktér spektrometru
 - Společně Nobelova cena 1915 – analýza struktury krystalů s využitím rentgenového záření



Rentgenová difraktometrie

- Braggova rovnice – interference fázově posunutých vln
– model „odrazu“ na soustavě rovnoběžných krystalových rovin – fyzikálně ekvivalentní k Laueovým rovnicím

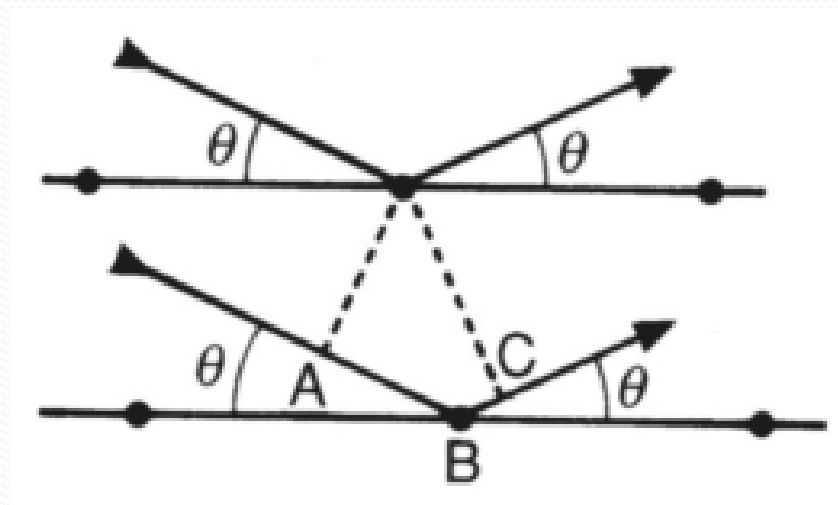
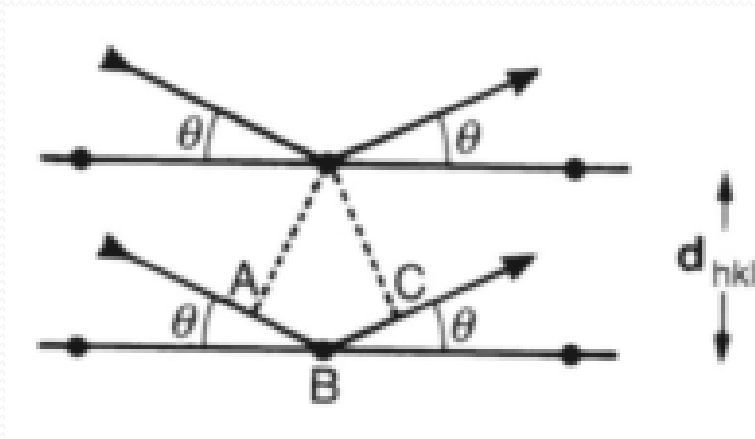
$$2d \sin \Theta = n \lambda \quad n=1,2,3\dots$$



Rentgenová difraktometrie

- Braggova rovnice – aplikovatelný bez ohledu na polohy atomů v rovinách – důležitá je pouze mezirovinná vzdálenost

$$2d \sin \Theta = n \lambda \quad n=1,2,3\dots$$



Rentgenová difraktometrie

– web simulace

Bragg's law - Google Chrome

Google

http://kr-01-032-pc1.physik.uni-erlangen.de/cgi-bin/discus/discus2.cgi?script=teach_bragg&P1=0.7&P2=&P3=0.0&P4=10&run=++RUN++&P5=0.75

Interactive Tutorial about Diffraction

Bragg's law

Wave length:

Distance between planes:

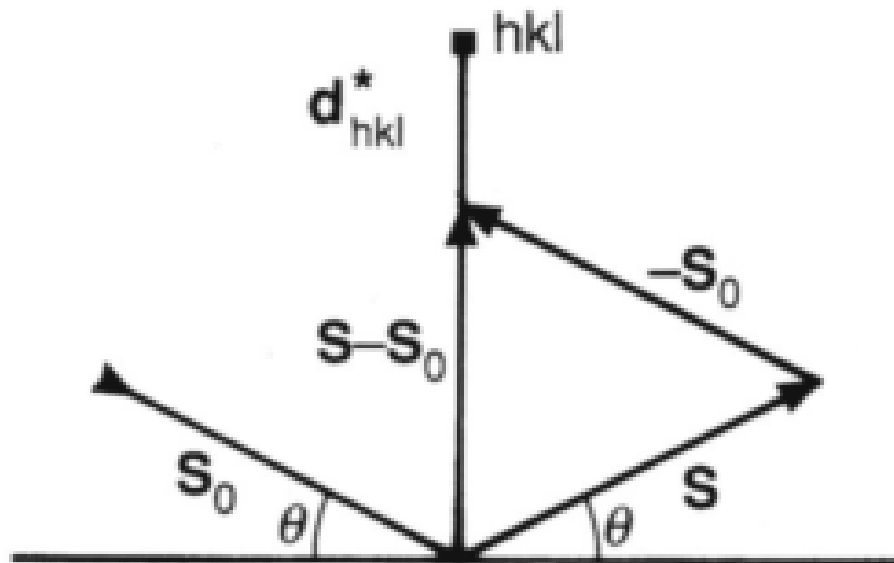
X-coordinate of atom on upper plane:

Theta:

Rentgenová difraktometrie

$$2d \sin \theta = n \lambda \quad n=1,2,3\dots$$

- Braggova rovnice – vektorově
- $|\mathbf{s} - \mathbf{s}_0| = 2 \sin \theta$, $d_{hkl}^* = 1/d_{hkl}$
 - $\mathbf{s} - \mathbf{s}_0 / \lambda = \mathbf{d}_{hkl}^*$
- Konstruktivní interference - když vektor $\mathbf{s} - \mathbf{s}_0 / \lambda$ souhlasí s vektorem \mathbf{d}_{hkl}^*

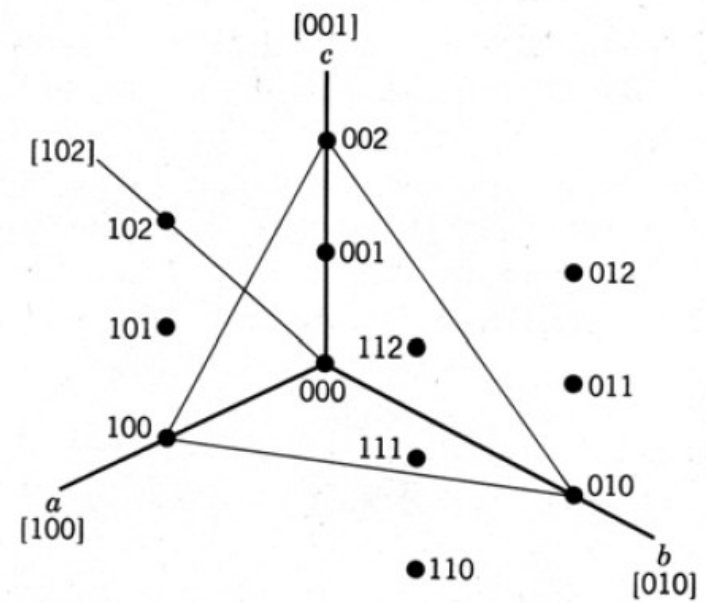


Rentgenová difraktometrie

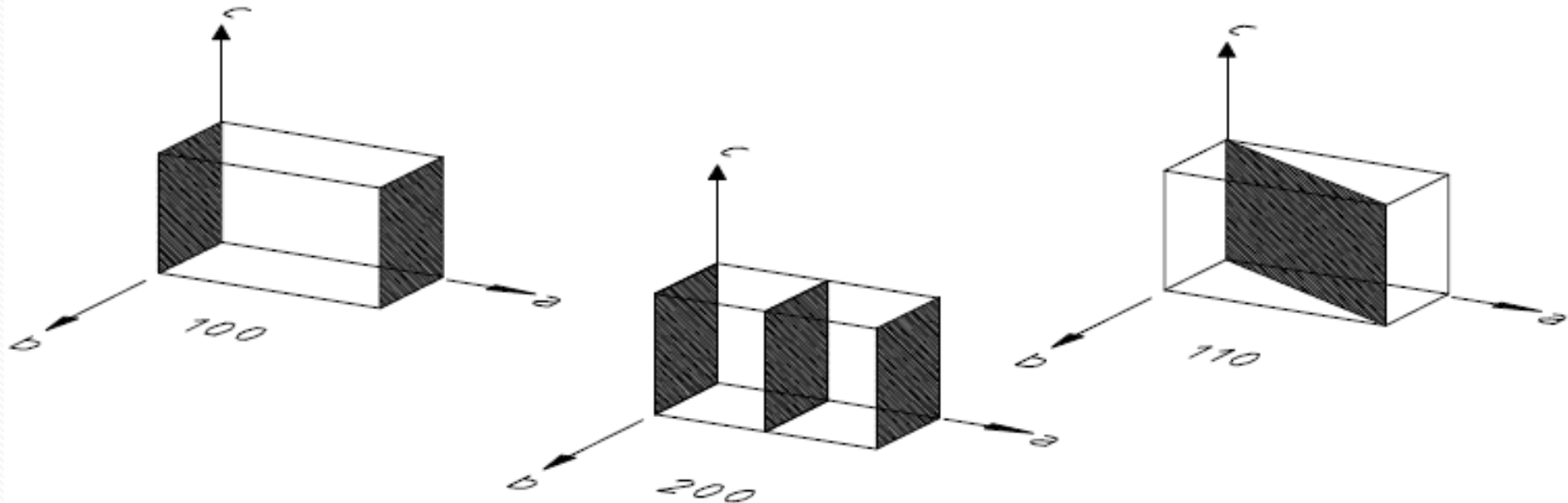
$$\sin \theta = n \lambda / 2d \quad n=1,2,3\dots$$

- The possible 2-THETA values where we can have reflections are determined by the unit cell dimensions.
- However, the intensities of the reflections are determined by the distribution of the electrons in the unit cell.
- The highest electron density are found around atoms. Therefore, the intensities depend on what kind of atoms we have and where in the unit cell they are located.
- Planes going through areas with high electron density will reflect strongly, planes with low electron density will give weak intensities.

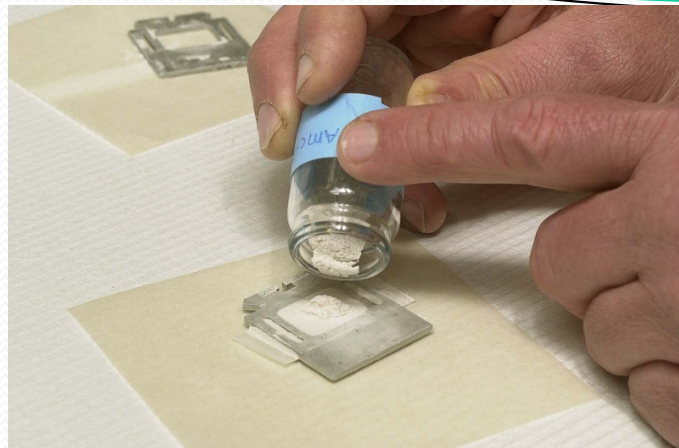
Rentgenová difraktometrie



- parametry – indexy - h, k, l – čísla daná protínáním os



Rentgenová difraktometrie

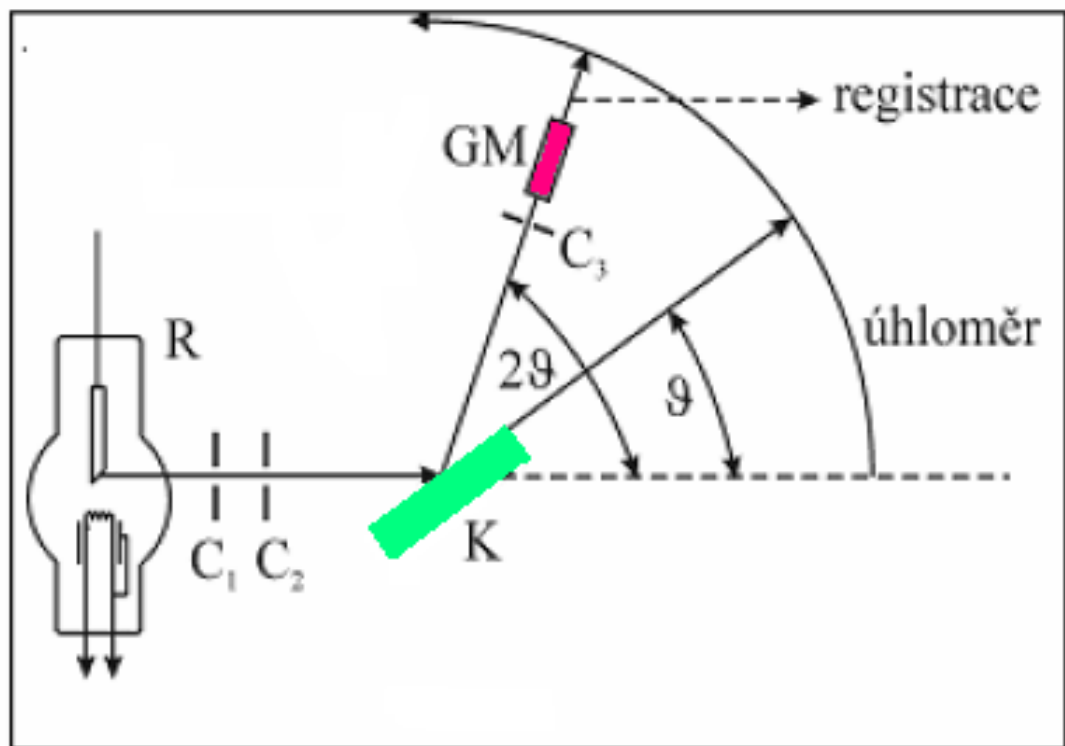


- vzorky

- **PRÁŠKOVÉ** – polykrystalické – identifikace fází ve vzorku na principu „otisku palce“
 - Pokud možno vzorek s rovným a hladkým povrchem, rozetřený prášek – průřez částic 2 – 5 μm
 - Ideálně - homogenní vzorek s náhodnou distribucí orientace krystalitů – prášek vtlačen do držáku vzorků (běžně stovky mg)
- **MONOKRYSTAL** – běžné požadována velikost – průřez – cca 0,3 mm – určení molekulární struktury nových či dosud nepopsaných látek

Rentgenová difraktometrie

- Princip jednoduchého spektrometru



- Úhlová disperze RTG spektrometru

$$\frac{\partial \vartheta}{\partial \lambda} = \frac{n}{2d \cos \vartheta}$$

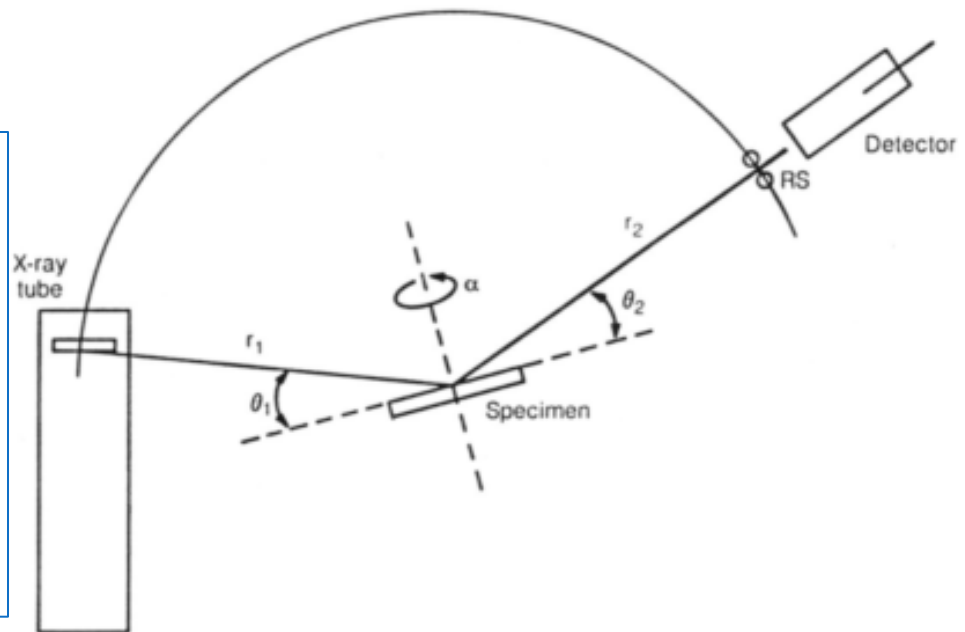
- přímá úměra k řádu difrakce
- intenzita ovšem klesá s řádem

Rentgenová difraktometrie

- Obvykle snímána spektra 1. řádu – pouze pro rozlišení detailů spektra vyšších řádů – výrazné prodloužení doby expozice
- Mezní dosažitelné rozlišení určeno rozlišovací schopností přístroje
- Bragg-Brentanův difraktometr

$$\lambda / \delta\lambda$$

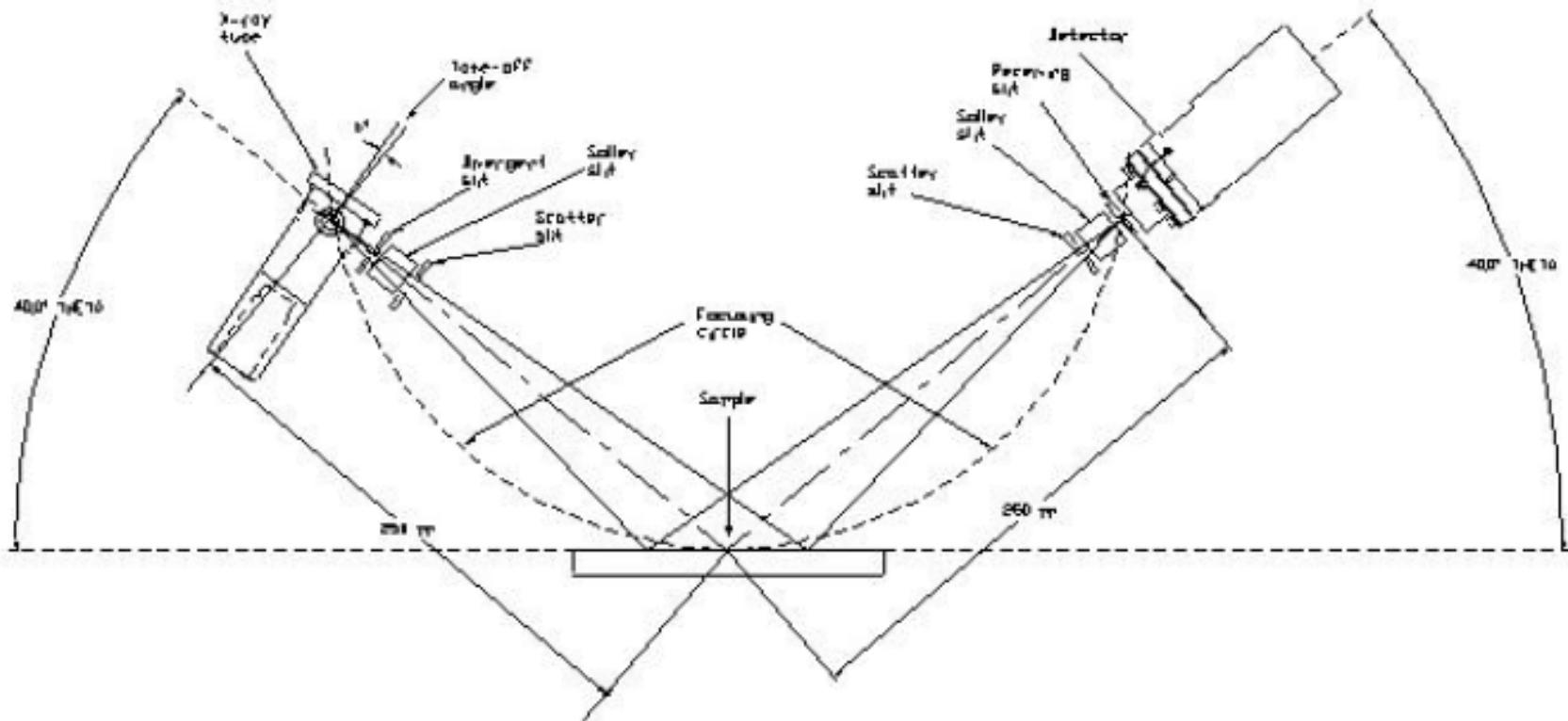
For the THETA:2-THETA goniometer, the X-ray tube is stationary, the sample moves by the angle THETA and the detector simultaneously moves by the angle 2-THETA.



Rentgenová difraktometrie

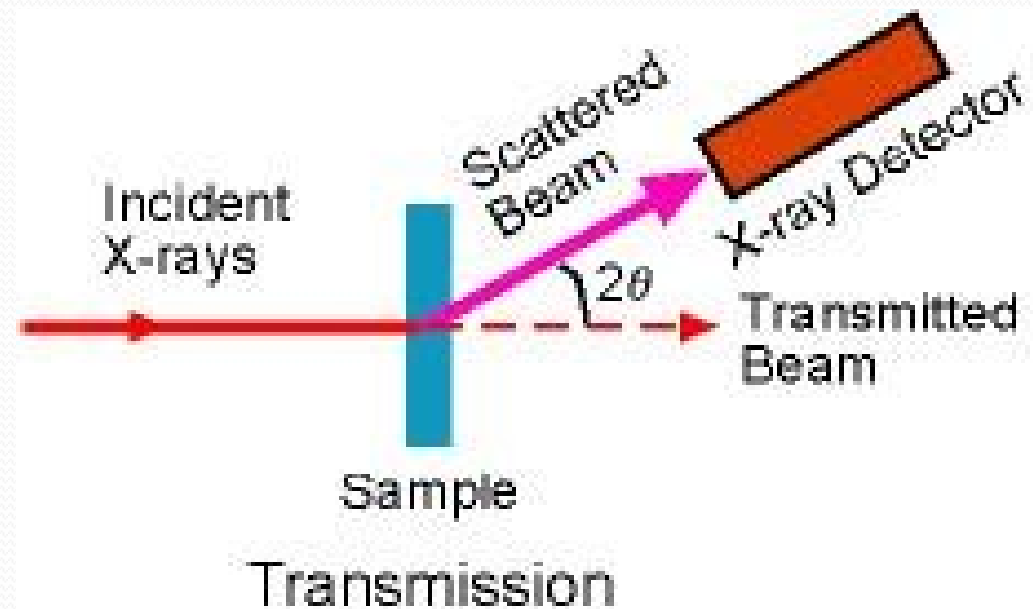
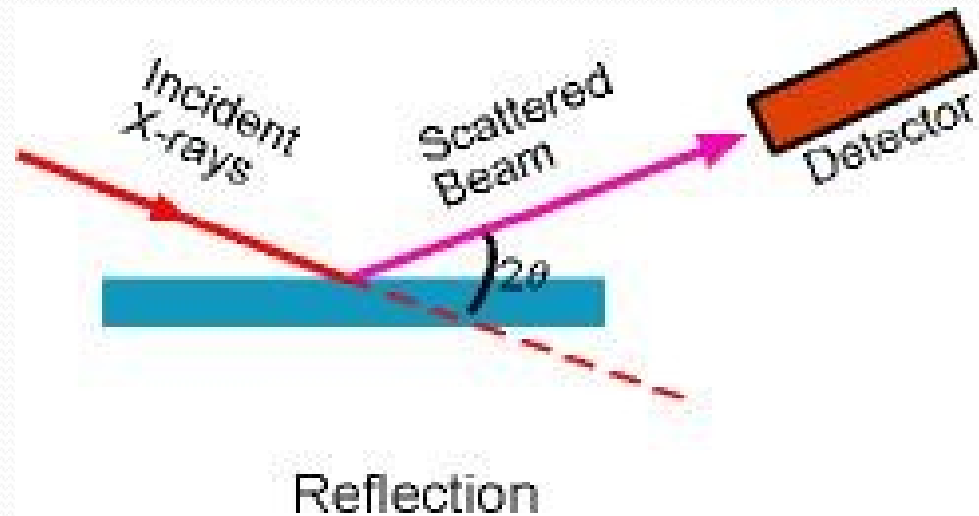
- Bragg-Brentanův difraktometr
- For the THETA:THETA goniometer, the sample is stationary in the horizontal position, the x-ray tube and the detector both move simultaneously over the angular range THETA.

Bragg Brentano THETA:THETA Setup



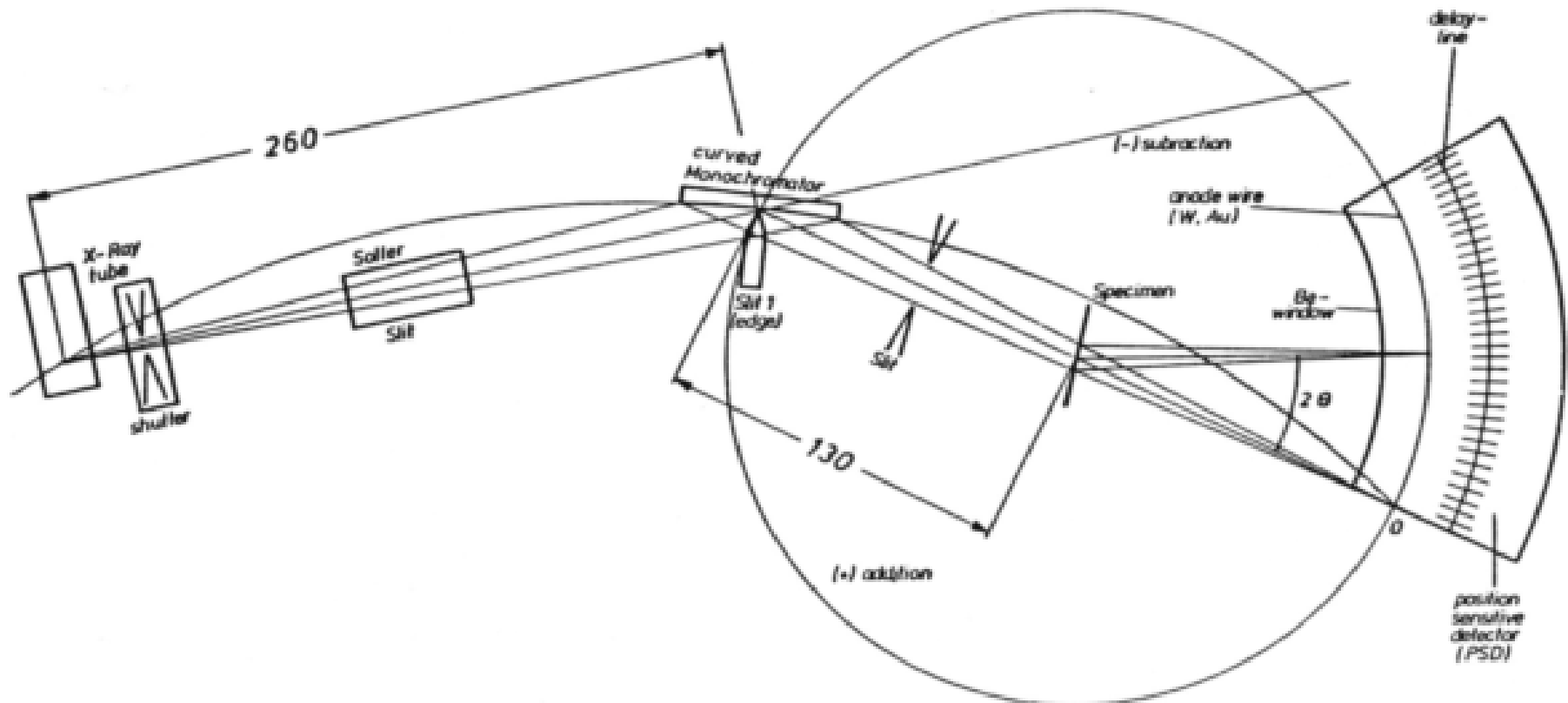
Rentgenová difraktometrie

- PRÁŠKOVÁ

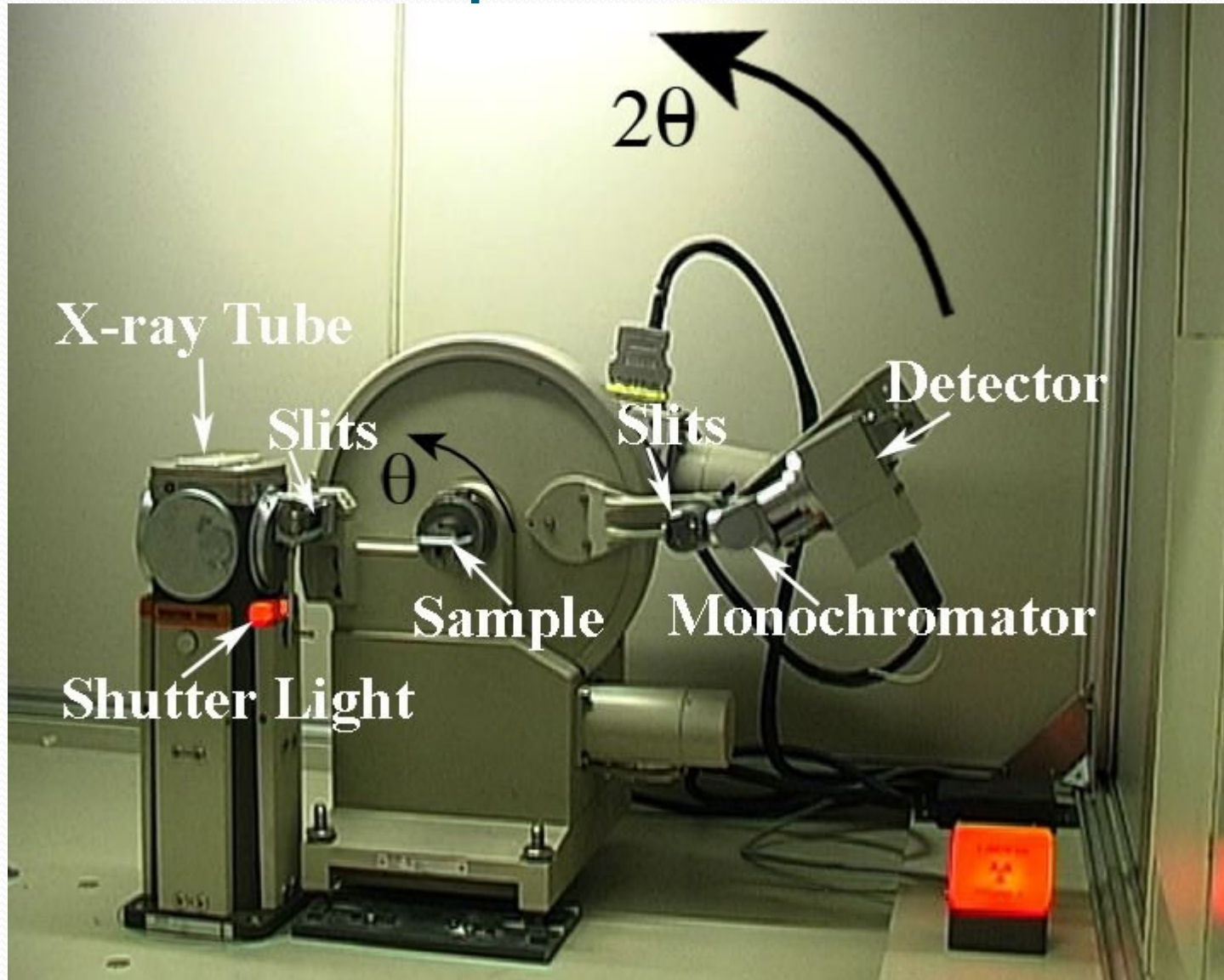


Rentgenová difraktometrie

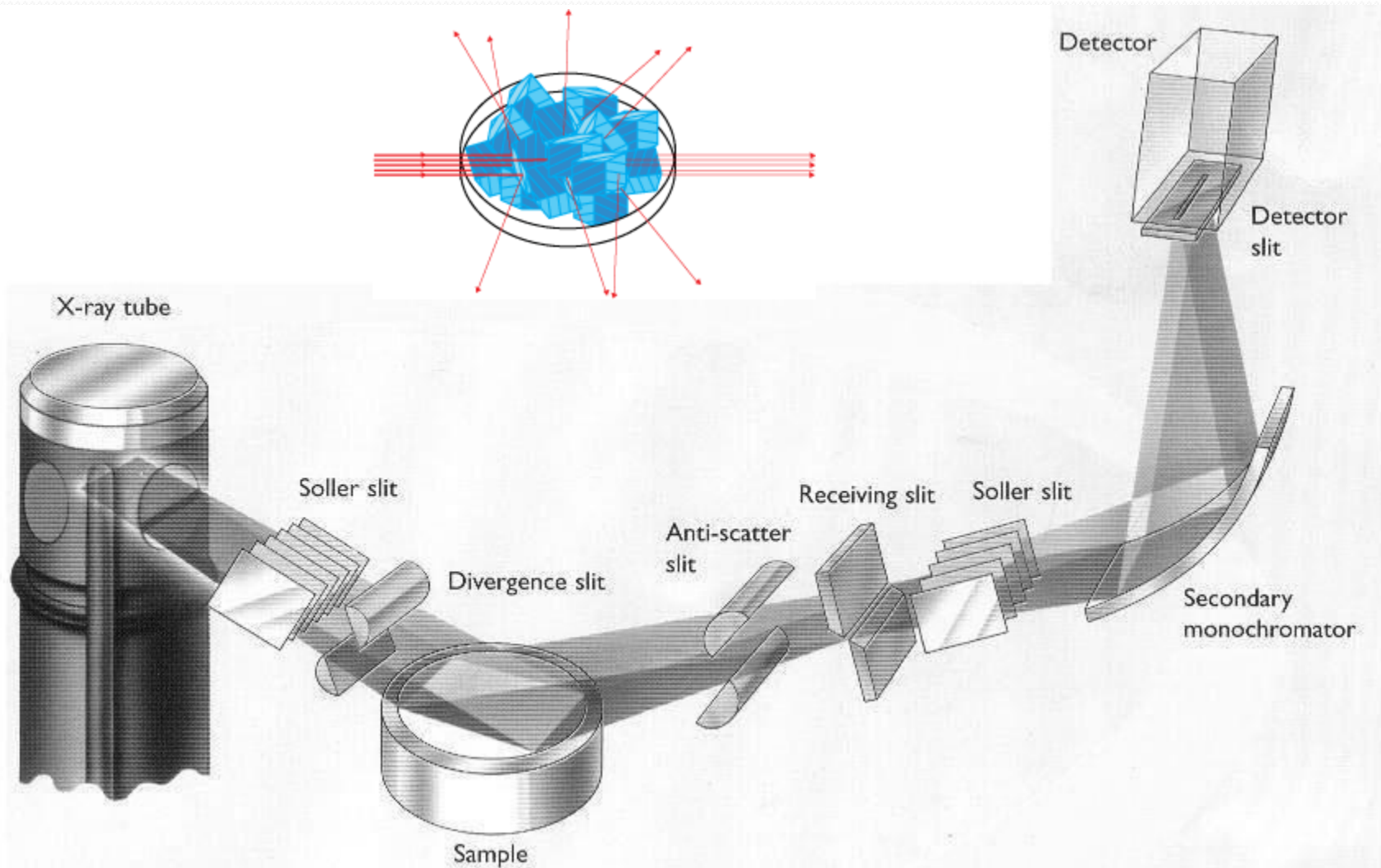
- Transmisní uspořádání difraktometru s primárním monochromátorem (pro práškovou difraktometrii) (obecně monochromátor v primárním či difraktovaném svazku)



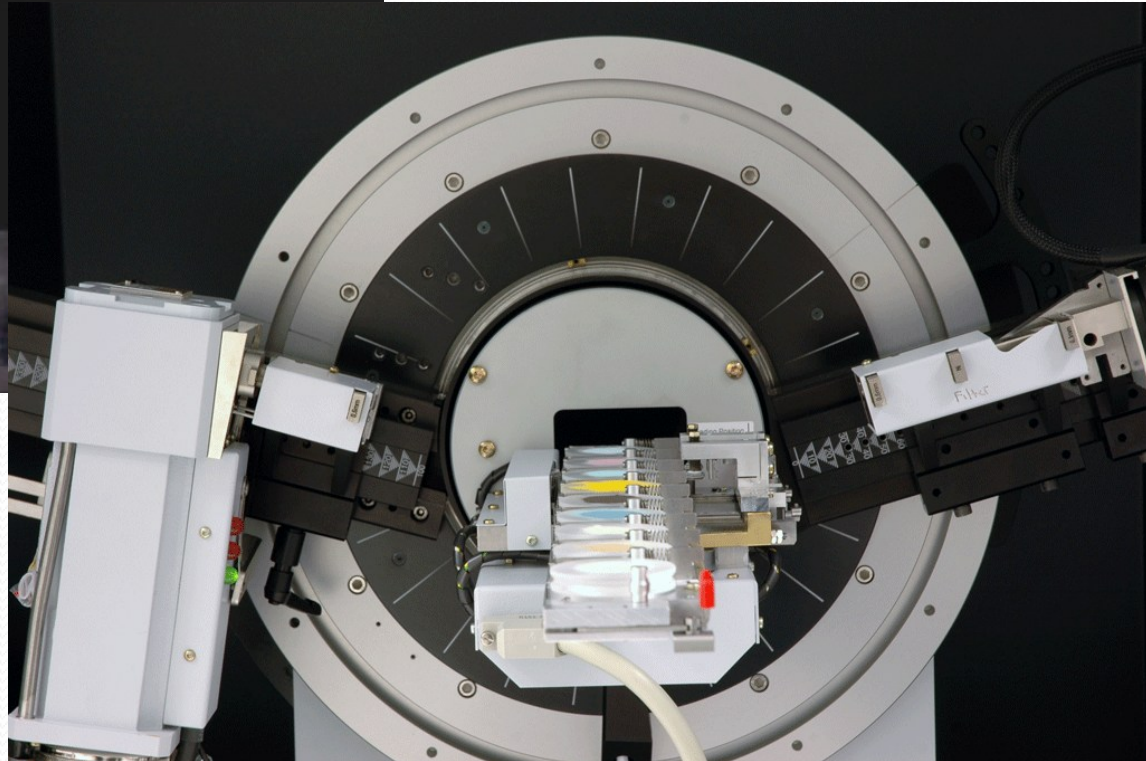
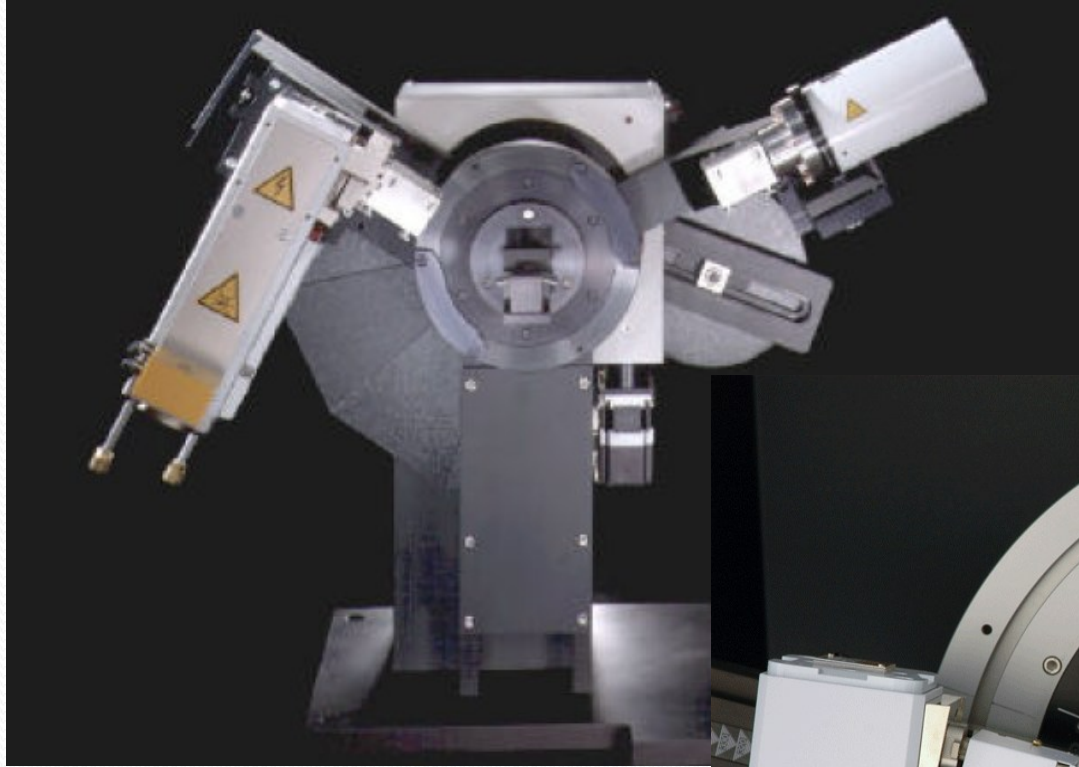
Rentgenová difraktometrie prášková



Rentgenová difraktometrie prášková



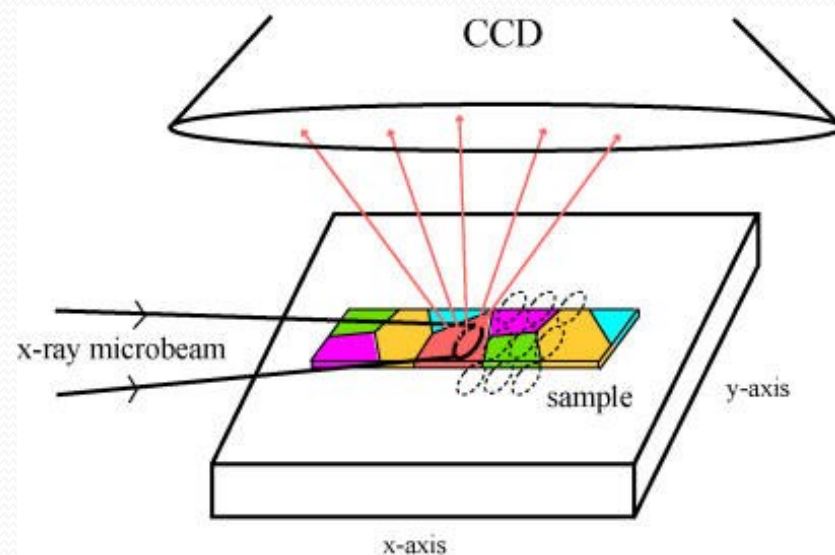
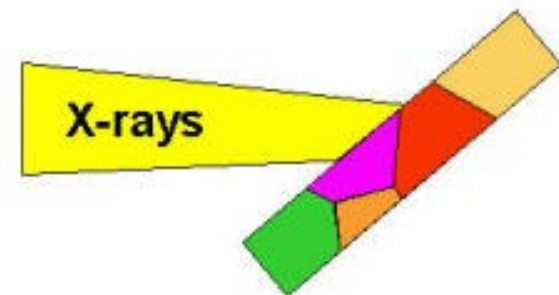
Rentgenová difraktometrie prášková



Rentgenová difraktometrie



- Ozařovaná plocha na vzorku – běžně mm^2 , pokud se nejedná o mikroanalýzu
- Intenzita ozařování – řádově stovky W/mm^2
- **RTG – mikrodifrakce** – ozařovaná plocha běžně μm^2 i méně (synchrotronové záření) – mikrostruktura materiálů – lokální změny struktury



Rentgenová difraktometrie

• RTG – mikrodifrakce

Material analysis with X-ray microdiffraction

F. Friedel*¹, U. Winkler¹, B. Holtz¹, R. Seyrich², and H.-J. Ullrich²

Cryst. Res. Technol. **40**, No. 1/2, 182 – 187 (2005) / DOI 10.1002/crat.200410323

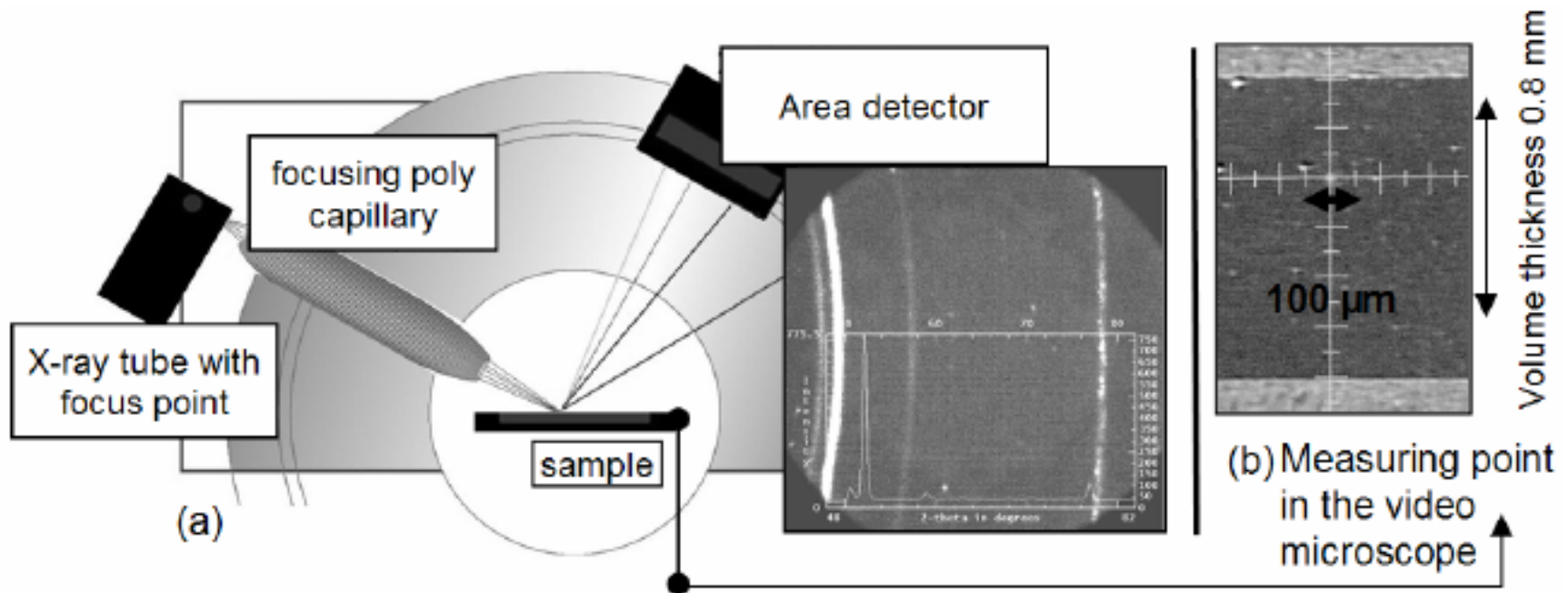


Fig. 2 Principle of X-ray microdiffraction with focusing polycapillary and area detector (source: Bruker AXS) (a), View by the video microscope of the microdiffraction equipment of the embedded and polished cross section (b).

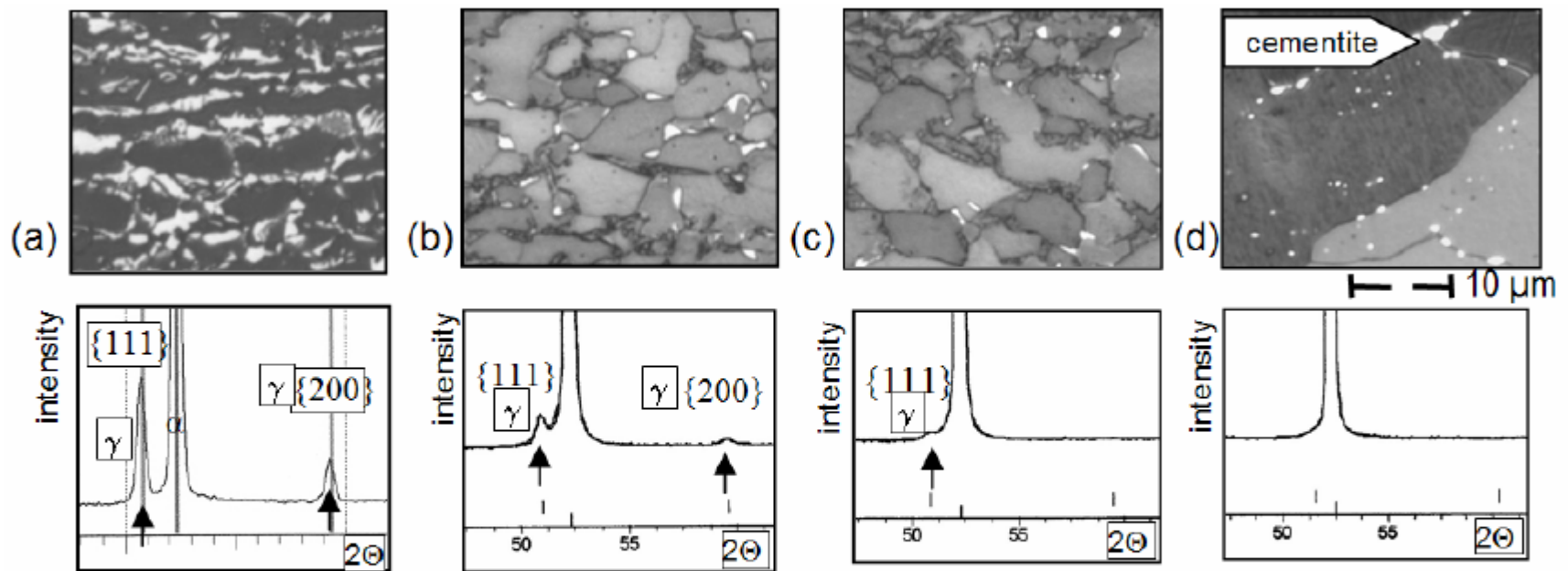
Röntgenová difraktometrie

• RTG – mikrodifrakce

Material analysis with X-ray microdiffraction

F. Friedel^{*1}, U. Winkler¹, B. Holtz¹, R. Seyrich², and H.-J. Ullrich²

Cryst. Res. Technol. **40**, No. 1/2, 182 – 187 (2005) / DOI 10.1002/crat.200410323

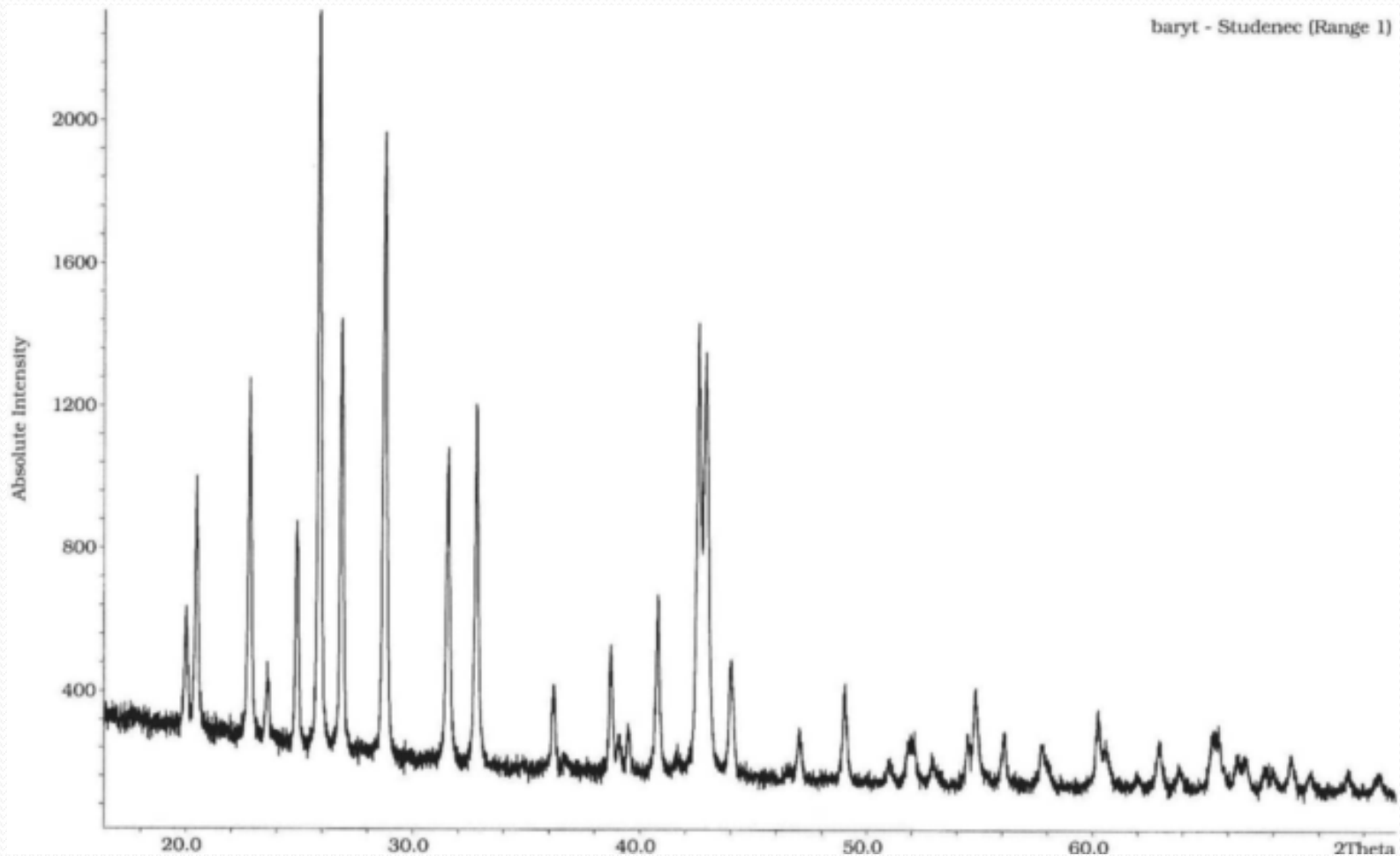


16 % residual austenite 4 % residual austenite 1 % residual austenite no residual austenite

Fig. 3 Measurement of residual austenite in the structure of a RA-steel (a), DP-steel (b) and (c) as well as distinction of the residual austenite as "white phase in the KLEMM etch process" of cementite in a conventional steel (d).

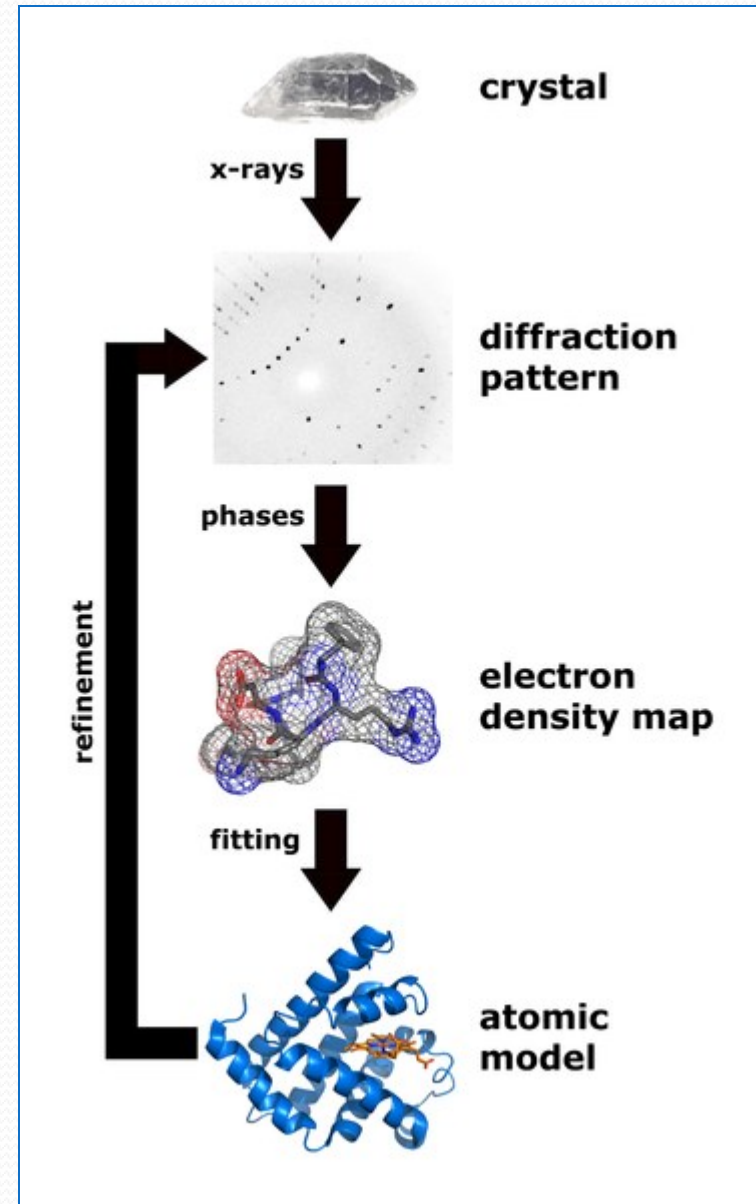
Rentgenová difraktometrie “prášková”

- Difraktogram



Rentgenová difraktometrie

- Kroky analýzy v RTG difraktometrii
- 1) měření difraktogramu
- 2) vyhodnocení - určení poloh a intenzit difrakcí (píků)
- 3) indexování difrakcí (h, k, l)
- 4) parametry základní buňky



Rentgenová difraktometrie

- Kroky analýzy v RTG difraktometrii
- vyhodnocení - určení poloh a intenzit difrakcí (píků)
- přípravné kroky
- vyhlazení záznamu (proklady metodou nejmenších čtverců)
- odečtení pozadí
- vyhodnocení záznamu 2. derivace

- zhodnocení instrumentálních vlivů (aberrací) – instrumentální justace, neinstrumentální korekce, metoda vnitřního standardu

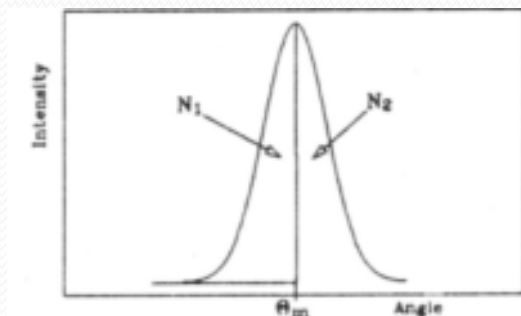
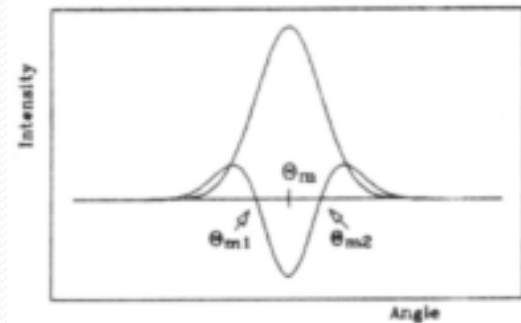
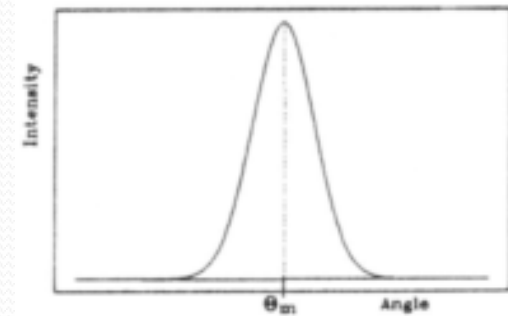
Rentgenová difraktometrie

- Kroky analýzy v RTG difraktometrii
- vyhodnocení - určení poloh a intenzit difrakcí (píků)
- maximum intenzity

- střední poloha mezi inflexními body

- těžiště difrakční linie

- proložení analytické funkce



Rentgenová difraktometrie

- Vyhodnocení - určení poloh a intenzit difrakcí (píků)



- proložení analytické funkce – profilové funkce

- Gaussova

$$V(x; \sigma, \gamma) = \int_{-\infty}^{\infty} G(x'; \sigma) L(x - x'; \gamma) dx'$$

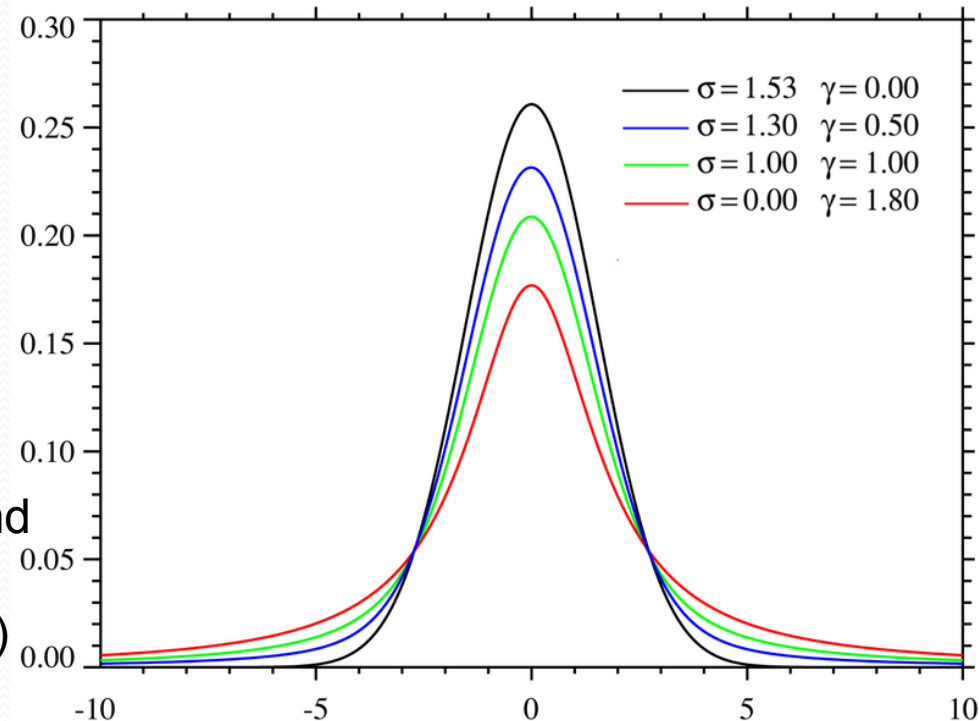
- Lorentzova

- Pearsonova

- Voigtova – konvoluce G & L

- pseudoVoigtova

Plot of the centered Voigt profile for four cases. Each case has a full width at half-maximum of very nearly 3.6. The black and red profiles are the limiting cases of the Gaussian ($\gamma = 0$) and the Lorentzian ($\sigma = 0$) profiles respectively.



Rentgenová difraktometrie

- The X-ray diffraction pattern of a pure substance is like a fingerprint of the substance.
- The powder diffraction method is thus ideally suited for characterization and identification of polycrystalline phases.
- Today about 50,000 inorganic and 25,000 organic single component, crystalline phases, diffraction patterns have been collected and stored on magnetic or optical media as standards. The main use of powder diffraction is to identify components in a sample by a search/match procedure. Furthermore, the areas under the peak are related to the amount of each phase present in the sample.

Rentgenová difraktometrie

- International Center Diffraction Data (ICDD), formerly known as (JCPDS) Joint Committee on Powder Diffraction Standards, is the organization that maintains the database of inorganic and organic spectra. The database is available from diffraction equipment manufacturers or from ICDD direct.
- <http://www.icdd.com/>
- The database is exhaustive, over 500,000 entries as of 2006; computer algorithms allow rapid peak matching. The organization was founded in 1941 as the Joint Committee on Powder Diffraction Standards (JCPDS).

Rentgenová difraktometrie

- **Aplikace**
- Identifikace – pro krystalické fáze – na základě databáze,
- Studium teplotních změn, vlivu tlaku atp.
- Struktura nových látek
- Míra krystalinity materiálů (polymerů)
- Analýza textury – preferenční orientace v polykrystalických materiálech („preferred crystallographic orientation in a polycrystalline material“)

Rentgenová difraktometrie

Anatase R060277 - RRUFF... x

http://rruff.info/Anatase/R060277 Zadejte hledaný text

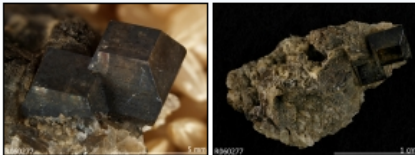
Save Page as PDF Gmail: E-mail od Google Introductions to Man... AXA Česká Republika ... Wavelength-dispersiv... Introduction to the si...

RRUFF Home | UA Mineralogy | Caltech Mineralogy | The IMA Mine

RRUFF Search **Sample Data** Search **References** **About RRUFF** **Contact Us**

Anatase R060277

[Browse S](#)
<< Previous | Back to Search Res



Name: Anatase
RRUFF ID: R060277
Ideal Chemistry: TiO_2
Locality: Taftan, near Dalbandi, Baluchistan Province, Pakistan
Source: Herb Obodda 064 [view label]
Owner: RRUFF
Description: Dark brown tetragonal tabular crystals
Status: The identification of this mineral is confirmed by single-crystal X-ray diffraction and c
analysis.

Quick search: [All Anatase samples (2)]

POWDER DIFFRACTION

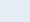
RRUFF ID: R060277.9

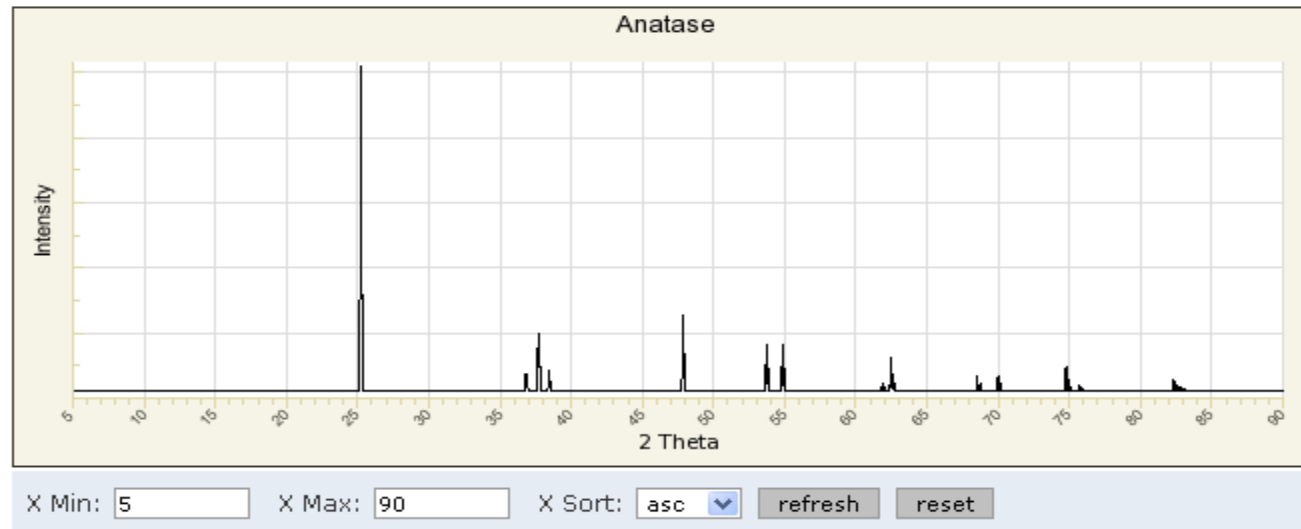
Sample Description: Single crystal, powder profile is calculated

Cell Refinement Output: a: 3.799(2)Å b: 3.799(2)Å c: 9.539(6)Å

alpha: 90° beta: 90° gamma: 90° **Volume:** 137.67(5) **Crystal System:** tetragonal

DOWNLOADS:

-  DIF File
-  X-ray Data (XY - RAW) 
-  RRUFF File



Rentgenová difraktometrie

Anatase R060277 - RRUFF... x

http://ruff.info/Anatase/R060277 Zadejte hledaný text

Save Page as PDF Gmail: E-mail od Google Introductions to Man... AXA Česká Republika ... Wavelength-dispersiv... Introduction to the si...

RRUFF Home | UA Mineralogy | Caltech Mineralogy | The IMA Mine

RRUFF

Search **Sample Data** Search **References** **About RRUFF** **Contact Us**

Anatase R060277

Browse S
<< Previous | Back to Search Res



Name: Anatase
RRUFF ID: R060277
Ideal Chemistry: TiO_2
Locality: Taftan, near Dalhandi, Baluchistan Province, Pakistan

RAMAN SPECTRUM

RRUFF ID:

Sample Description: Sample is oriented and mounted on a pin

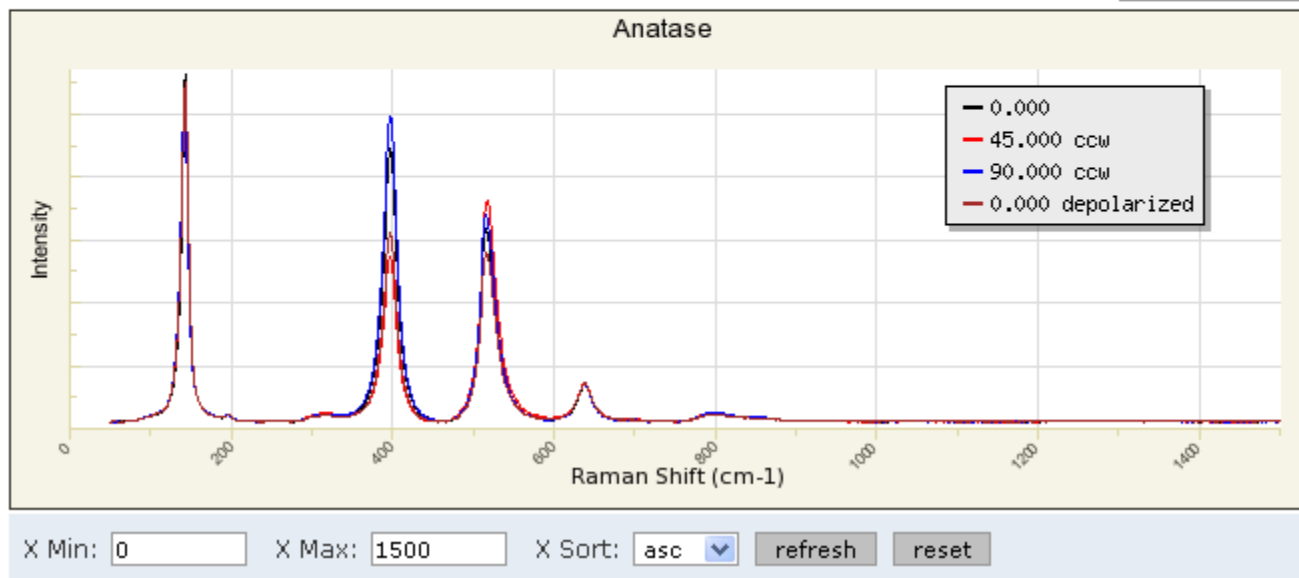
Pin ID: L01480

Orientation: Laser parallel to c^* (0 0 1). Fiducial mark perpendicular to laser is parallel to [1 1 0].

DOWNLOADS:

To download sample data,
please select a specific
orientation angle.

Direction of polarization of laser relative to fiducial mark:



Rentgenová difraktometrie

Yttrium aluminum garnet - ... x Yttriumaluminumgarnet_X... x

http://rruff.info/yttrium%20aluminum%20garnet/display=default/

Save Page as PDF Gmail: E-mail od Google Introductions to Man... AXA Česká Republika ... Wavelength-dispersiv... Introduction to the si...

RRUFF Home | UA Mineralogy | Caltech Mineralogy | The IMA Mineral

RRUFF 

[Search Sample Data](#) [Search References](#) [About RRUFF](#) [Contact Us](#)

Yttrium aluminum garnet X090003

**Name:** Yttrium aluminum garnet
RRUFF ID: X090003
Ideal Chemistry: $Y_3Al_2(AlO_4)_3$
Locality: Synthetic
Source: Gemological Institute of America 15735
Owner: GIA
Description: Faceted colorless gemstone, 1.42 ct
Status: The identification of this mineral has only been confirmed by single-crystal X-ray diffraction.

Rentgenová difraktometrie

RAMAN SPECTRUM

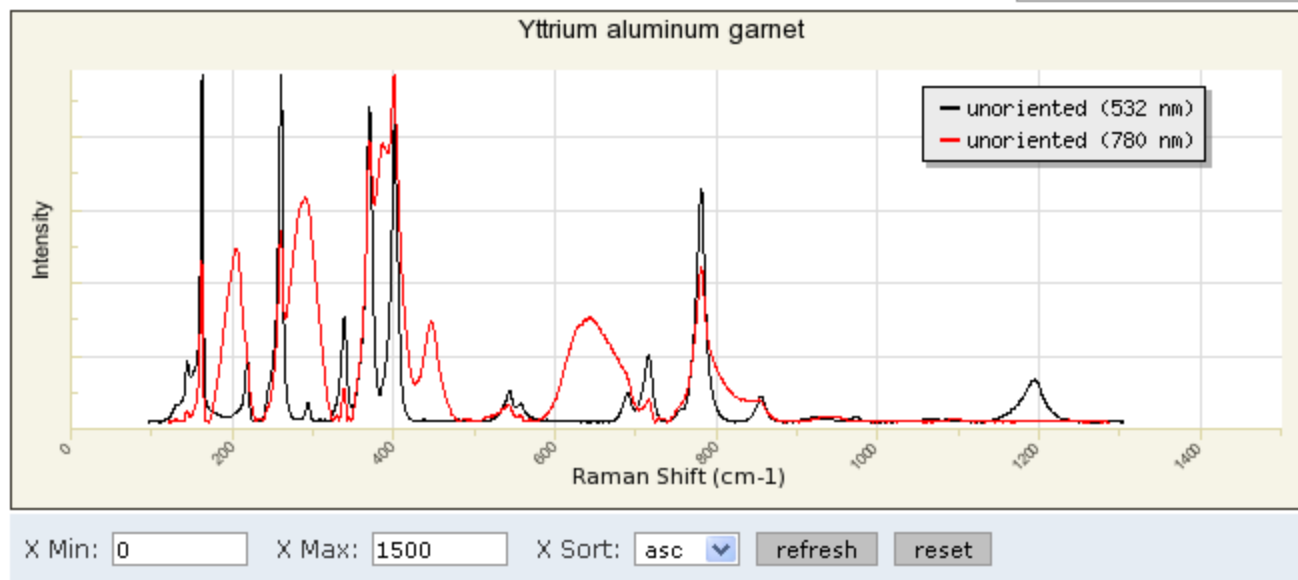
RRUFF ID: X090003

Sample Description: Unoriented sample

DOWNLOADS:

To download sample data, please select a specific orientation angle.

Direction of polarization of laser relative to fiducial mark: all data



Rentgenová difraktometrie

POWDER DIFFRACTION

RRUFF ID: X090003.9

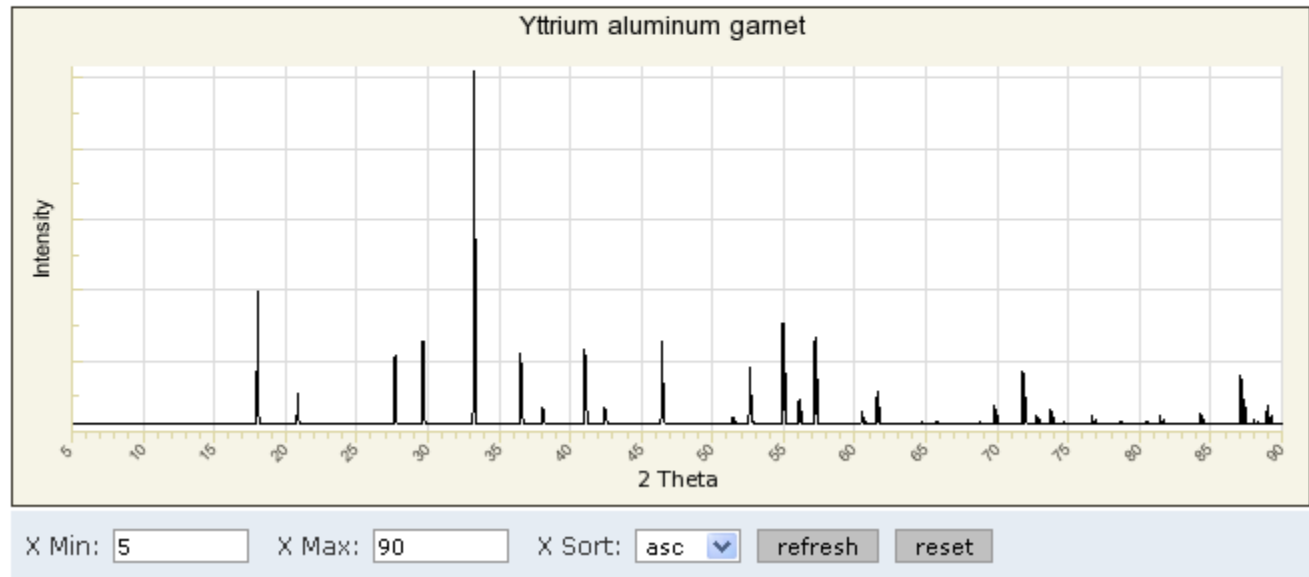
Sample Description: Single crystal, powder profile is calculated

Cell Refinement Output: a: 12.041(7)Å b: 12.041(7)Å c: 12.041(7)Å

alpha: 90° beta: 90° gamma: 90° Volume: 1745.7(1) Crystal System: cubic

DOWNLOADS:

-  DIF File
-  X-ray Data (XY - RAW) 
- RRUFF File



<http://rruff.info/yttrium%20aluminum%20garnet/display=default/>

Rentgenová difraktometrie



Non-destructive analysis of cultural heritage artefacts from Andalusia, Spain, by X-ray diffraction with Göbel mirrors

A. Duran*, L.K. Herrera, M.C. Jimenez de Haro, A. Justo, J.L. Perez-Rodriguez

Talanta 76 (2008) 183–188

Materials Science Institute of Seville (CSIC-Seville University), Avda Americo Vespucio, s/n. 41092 Seville, Spain

The characterization of the phases present in artefacts has been normally carried out using XRD (Bragg–Brentano geometry) that requires sampling from artworks, being a destructive technique. However, X-ray diffraction with Göbel mirrors permits directly to study rough artefacts without sampling. Grazing incidence attachments can be used to characterize as much the superficial layer as the underlying ones in flat samples to obtain information about the depth profile of some samples. The combination of Göbel mirrors and measure at low fixed incidence angles allow to obtain information about the depth profile of bent samples.

This work reports the alteration processes on the surface of the following cultural heritage artefacts: a rivet and a nail extracted from Pardon Gateway, located in the North facade of Mosque-Cathedral of Cordoba; a Roman arrow and a button from a Roman jacket obtained from an excavation in Baena (Cordoba); organ pipe from Cathedral of Zaragoza; lead seals from Seville City Hall collection.

The main objective of this paper is the study through a totally non-destructive analytical method, X-ray diffraction with Göbel mirrors, of the superficial alteration of some metallic artefacts from cultural heritage. This knowledge allows us the election of appropriate methods to carry out the restoration of these artefacts.

Rentgenová difraktometrie



Non-destructive analysis of cultural heritage artefacts from Andalusia, Spain, by X-ray diffraction with Göbel mirrors

A. Duran*, L.K. Herrera, M.C. Jimenez de Haro, A. Justo, J.L. Perez-Rodriguez

Talanta 76 (2008) 183–188

Materials Science Institute of Seville (CSIC-Seville University), Avda Americo Vesputio, s/n. 41092 Seville, Spain

Graded Multilayer Optics (“Göbel-Mirrors”) have proved as very useful beam conditions for parallel-beam diffraction without sampling.

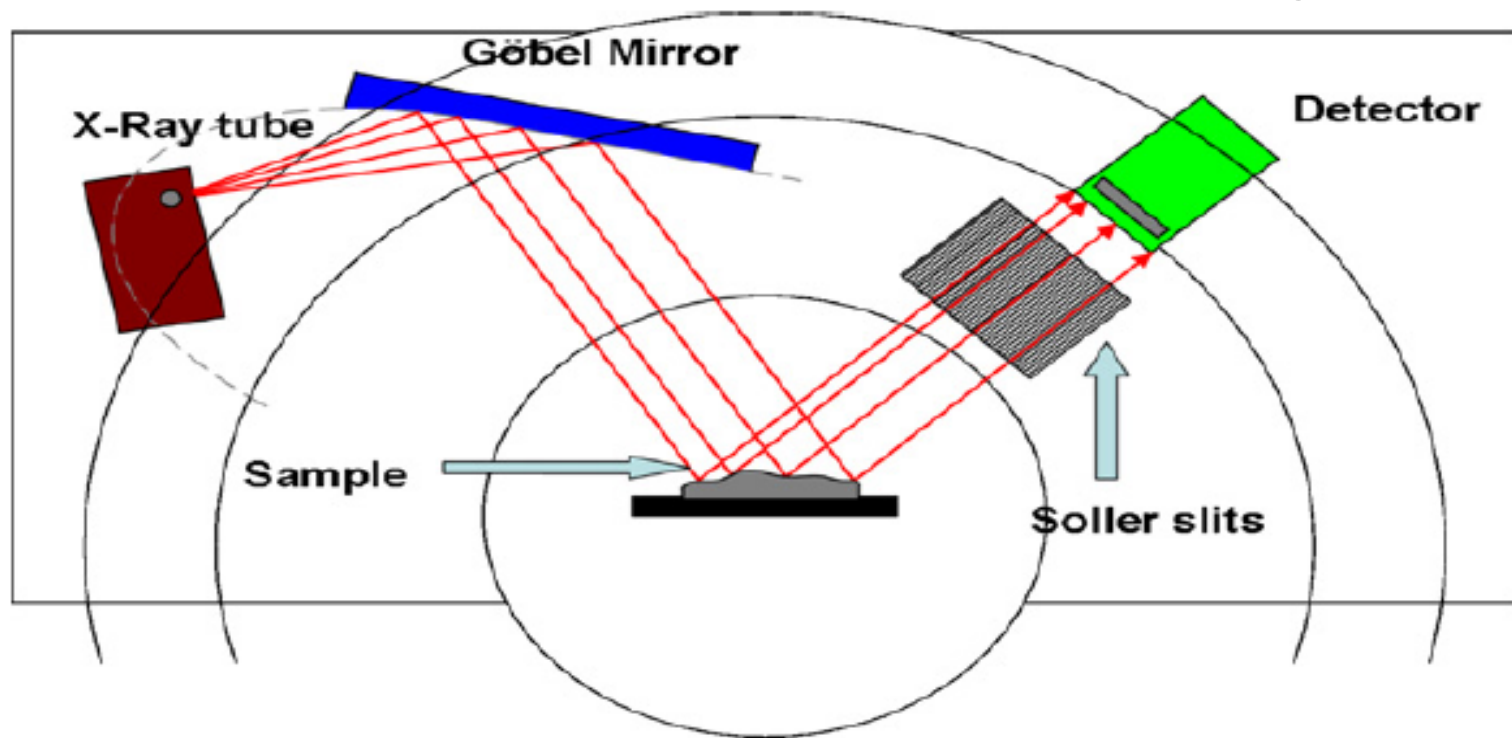


Fig. 1. Experimental procedure for non-destructive analysis by X-ray diffraction with Göbel mirrors of artefacts belonging to cultural heritage.

Rentgenová difraktometrie



Non-destructive analysis of cultural heritage artefacts from Andalusia, Spain, by X-ray diffraction with Göbel mirrors

A. Duran*, L.K. Herrera, M.C. Jimenez de Haro, A. Justo, J.L. Perez-Rodriguez

Talanta 76 (2008) 183–188

Materials Science Institute of Seville (CSIC-Seville University), Avda Americo Vesputcio, s/n. 41092 Seville, Spain

The “Göbel-Mirrors” are a **device, based on a layered crystal**, which, mounted on a D-5000 Siemens diffractometer, transforms the primary divergent X-ray beam into a **highly brilliant, parallel beam**. If dimensions of an object are adequate (up to 60cm in bulk), it can be directly analyzed by XRD, without sampling. **Even a rough, irregular surface, both on flat and bent objects, is suitable for the analysis.**

The XRD analysis using Göbel mirrors is therefore, totally nondestructive and very useful to study artefacts from Cultural Heritage [5–7]. It can be obviously very adaptable to study the surfaces of these artefacts, giving information of **degradation and corrosion processes** and information about **pigments, ceramics, metals, patinas, crusts**, etc., used to manufactured artworks.

Rentgenová difraktometrie



Non-destructive analysis of cultural heritage artefacts from Andalusia, Spain, by X-ray diffraction with Göbel mirrors

A. Duran*, L.K. Herrera, M.C. Jimenez de Haro, A. Justo, J.L. Perez-Rodriguez

Materials Science Institute of Seville (CSIC-Seville University), Avda Americo Vespucio, s/n. 41092 Seville, Spain

Talanta 76 (2008) 183–188

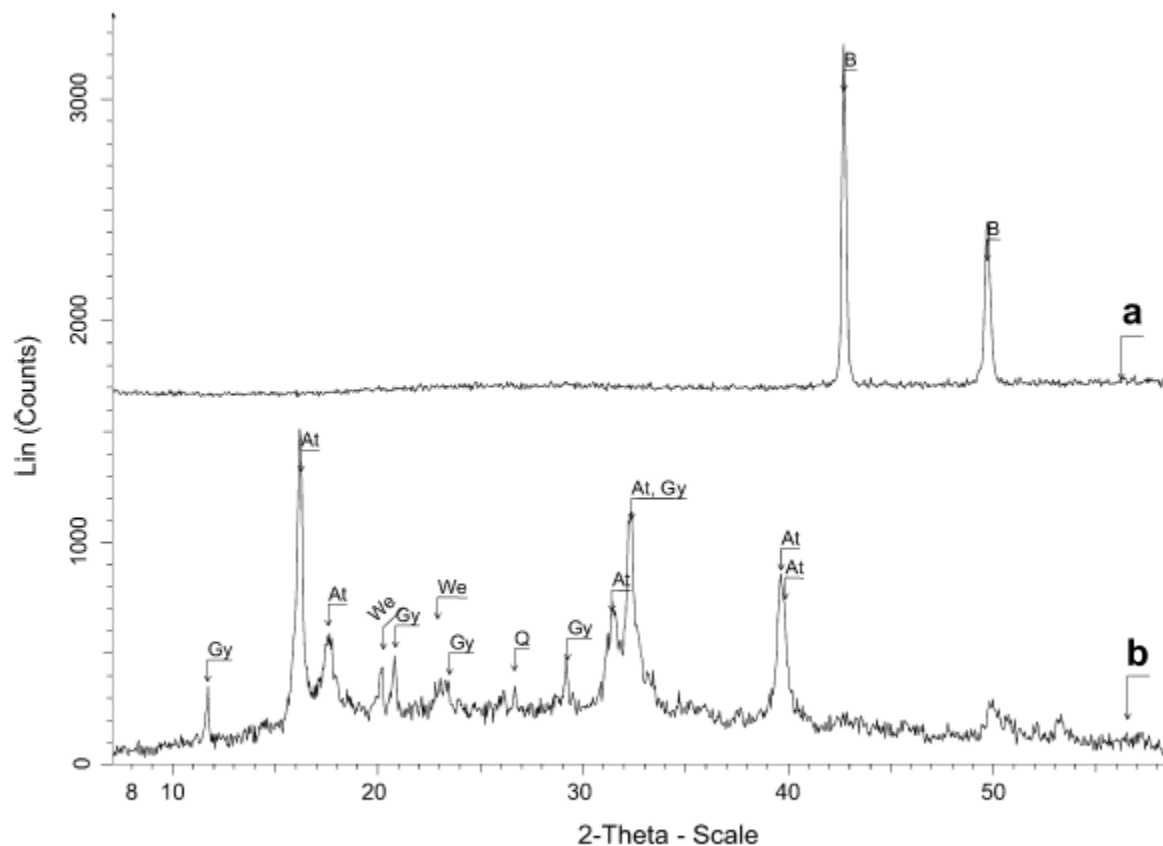


Fig. 3. X-ray diffraction pattern with Göbel mirrors of: (a) a rivet extracted from the Pardon Portico of the Mosque-Cathedral, corresponding to alpha bronze. (b) Superficial product on the altered bronze of the Portico, corresponding to atacamite (At), gypsum (Gy), quartz (Q) and weddellite (We).

Rentgenová difraktometrie



Non-destructive analysis of cultural heritage artefacts from Andalusia, Spain, by X-ray diffraction with Göbel mirrors

A. Duran*, L.K. Herrera, M.C. Jimenez de Haro, A. Justo, J.L. Perez-Rodriguez

Talanta 76 (2008) 183–188

Materials Science Institute of Seville (CSIC-Seville University), Avda Americo Vespucio, s/n. 41092 Seville, Spain

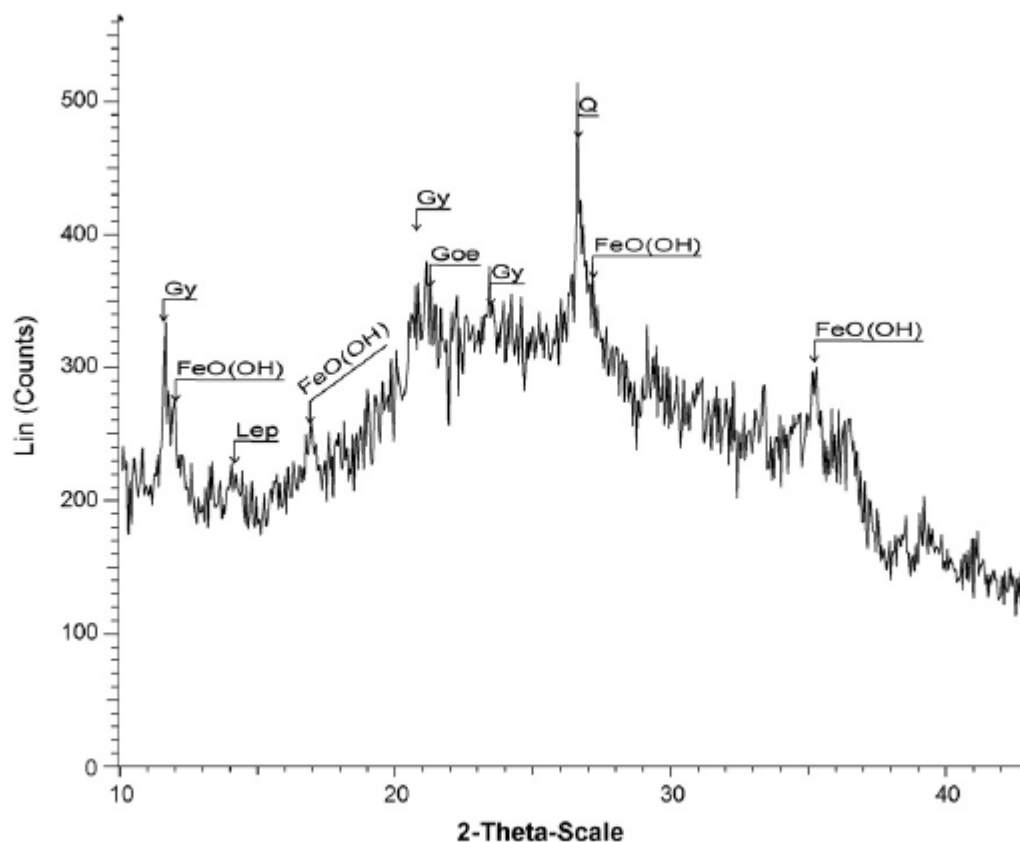


Fig. 4. X-ray diffraction pattern with Göbel mirrors of the altered iron nail of the Mosque-Cathedral of Cordoba, showing the presence of goethite (Goe), lepidocrocite (Lep), [FeO(OH)], gypsum (Gy) and Quartz (Q).

Rentgenová difraktometrie

The characterization of artefacts of cultural heritage
significance using physical techniques

Radiation Physics and Chemistry 74 (2005) 426–442

D.C. Creagh

Cultural Heritage Research Centre, Division of Science and Design, University of Canberra, Canberra ACT 2601, Australia

All societies attempt to preserve their cultural heritage because it is this that gives them their identity. How artefacts are identified as being of significance to society, and how to preserve these for posterity, depend on the sophistication of those societies, their wealth, and the determination of members of the societies to preserve their past. If conservation or restoration measures are being undertaken complex analytical experiments must be undertaken beforehand to ensure that the work is being undertaken in an appropriate manner. These investigations may employ electromagnetic (IR, VIS, UV, X-ray, γ -ray) or particulate (electron, proton, neutron, and ion beams) radiation. The use of many of these techniques is described in this paper in experiments on Australian Aboriginal bark paintings, a suit of armour belonging to a famous Australian outlaw, and the degradation of colour motion picture film.

Table 1
Types of radiation used in the work described in this paper

Energy range (eV)	Particle type	Interaction	Technique	Used for the study of
0.5–4	em (photon)	Absorption Inelastic scatter Elastic scatter	FTIR Raman Photography	Pigments & binders Pigments & binders Appearance & shapes
5000–40,000	em (photon)	Absorption Absorption Elastic scattering	XRF Tomography SRXRD	Atomic composition Internal structure Crystalline structure
1000–200,000	e^- (electron)	Absorption Secondary emission Elastic scattering Elastic scattering	SEM/EDAX SEM/SEI SEM/BEI STEM	Atomic composition Surface morphology Surface morphology Crystalline type
5000–10,000	n^0 (neutron)	Elastic scattering	Diffraction	Crystalline structure

Kulturní dědictví

The characterization of artefacts of cultural heritage significance using physical techniques

Radiation Physics and Chemistry 74 (2005) 426–442

D.C. Creagh

Cultural Heritage Research Centre, Division of Science and Design, University of Canberra, Canberra A

2.1. IR and Raman spectroscopy

Fourier Transform Infra-Red (FTIR) spectrometers are commonly used in most laboratories for the analysis of materials. An infrared spectrometer analyses the frequency of the infrared photons absorbed by the sample. *Absorption* occurs in transitions between vibrational modes of crystal structures and molecules within the sample. Measurement of absorption provides identification of the molecular species present in the sample by means of *comparison* of the band characteristics of the unknown species with those of standard materials. Most functional groups such as O–H, N–H, C=O have characteristic localized modes allowing for their easy identification on different samples. Other techniques use scattering rather than absorption of IR radiation, in particular, inelastic or Raman scattering. This technique is used extensively for the analysis of pigments and binders (Edwards et al., 1991).

2.1.1. Raman micro-spectroscopy

Most of the incident radiation scattered by a sample is *scattered elastically*. However, a small part of the incoming radiation (approximately 1 part in 10^5) interacts with the sample and is *scattered inelastically* (Raman scattering) re-emerging with a different frequency (energy). A Raman spectrometer is configured to reject the elastically scattered, and accept only the inelastically scattered radiation. A Renishaw 2000 Raman microscope was used in this work with illuminating lasers operating at 632.8 and 780 nm. The choice of laser is dictated by the emission of fluorescence by the specimen. As will be seen later this swamps the weak

2.1.2. FTIR micro-spectrometry

FTIR and Raman spectroscopy are *complementary* techniques. Vibrations which are strong in a Raman spectrum are usually weak in an infrared spectrum and vice versa. Qualitatively, antisymmetric vibrational modes and vibrations due to polar bonds (such as O–H, N–H, C=O) generally exhibit prominent infrared bands, while Raman tends to arise from vibrations involving more symmetrical bonds (such as C=C, C–C, S–S). As with Raman spectroscopy, complete compound identification is possible with FTIR by comparing band characteristics of the unknown species with those in commercial or in inhouse computer databanks.

Kulturní dědictví

The characterization of artefacts of cultural heritage
significance using physical techniques

Radiation Physics and Chemistry 74 (2005) 426–442

D.C. Creagh

Cultural Heritage Research Centre, Division of Science and Design, University of Canberra, Canberra ACT 2601, Australia

2.2. Techniques using radiation in the visible region of the radiation spectrum

In many experiments conventional optical microscopy has been used. The micro-Raman, micro-FTIR techniques, and micro-X-ray fluorescence spectrometer use optical spectroscopy for preliminary examinations of the specimen and the location of regions of interest. As well, we have employed transmission optical microscopy to study the structure of bark samples.

2.3. Fluorescence analysis

2.3.1. Micro-fluorescence spectroscopy

Analyses such as those mentioned in the preceding paragraph can be made using the technique of X-ray fluorescence spectroscopy. In this technique the specimen is irradiated by an X-ray source. This radiation causes the ejection of electrons from the innermost electron shells of the atoms in the sample into the continuum, and the subsequent rearrangement of electrons within the atom causes emission of X-rays (characteristic X-rays). The spectrum that results is unique to the atom emitting the radiation.

2.3.2. γ -X fluorescence spectrometry

For very large specimens, and for specimens which cannot be removed from museum custody, analyses can be undertaken using a portable γ -X spectrometer. This is not a micro-spectrometer, and the beam diameter is fixed at 1 mm diameter. For the study of Joe Byrne's armour a Thermo Metallurgist Pro Mercury II Probe was used. This has two γ -ray sources: ^{109}Cd (4 mCi at 80 keV), ^{55}Fe (4.5 mCi at 6.40 keV). It is a hand-held device and in principle it can sample any surface in any orientation. A HgI_2 detector is used, operated at room temperature. The fluorescence spectrum acquires in the detector is amplified, passed through a multichannel analyzer, the output from which is fed into a lap-top computer. This contains programs which enable a full spectral analysis with full matrix corrections to be undertaken. The spectral lines are compared with an internal database for metals and alloys.

Kulturní dědictví

The characterization of artefacts of cultural heritage significance using physical techniques

Radiation Physics and Chemistry 74 (2005) 426–442

D.C. Creagh

Cultural Heritage Research Centre, Division of Science and Design, University of Canberra, Canberra ACT 2601, Australia

2.4. X-ray diffraction

2.4.1. Laboratory XRD

Studies of the crystal structure of Joe Byrne's armour were undertaken using a Scintag diffractometer fitted with a copper target tube, operating at 38 kV, 30 mA. The diffractometer was operated in the θ – θ mode with a step scan size of 0.050° . The detector was a liquid nitrogen cooled solid state detector, the output of which was amplified and processed by a multichannel analyzer. A window was set such that only $\text{CuK}\alpha_1$ radiation was detected. The $\text{CuK}\beta$ and fluorescence radiation was rejected.

- high intensity, especially if auxiliary bending devices such as wigglers and undulators are used (typically more than 10^8 more intense than a conventional laboratory source),
- emission over a broad spectral range (from IR to X-ray energies; “white” radiation),
- high directionality (because of relativistic effects the divergence of the beams are typically less than 2 mrad vertically, 7 mrad horizontally),
- linear polarization in the plane of the orbit.

2.4.2. Synchrotron radiation X-ray diffraction

The use of synchrotron radiation sources by materials scientists for cultural heritage studies is still comparatively new. Synchrotron radiation sources dedicated to the study of materials have been in existence for about 20 years. Synchrotrons which generate radiation in the X-ray region (the region used in most structural analyses) typically have energies greater than 2 GeV. For example: the Photon Factory at the Japanese Institute for High Energy Research, Tsukuba, Japan, operates with a circulating current of electrons (400 mA at 2.6 GeV) and produces useful maximum X-ray energies for a bending magnet in the range 4.5–20 keV; the Advanced Photon Source at Argonne, USA operates at 6 GeV and produces useful maximum X-ray energies in the range 4–80 keV).

2.5. Electron microscopy

2.5.1. Scanning electron microscopy

2.5.2. High resolution transmission electron microscopy

2.6. Neutron diffraction

Kulturní dědictví

The characterization of artefacts of cultural heritage
significance using physical techniques

Radiation Physics and Chemistry 74 (2005) 426–442

D.C. Creagh

Cultural Heritage Research Centre, Division of Science and Design, University of Canberra, Canberra ACT 2601, Australia

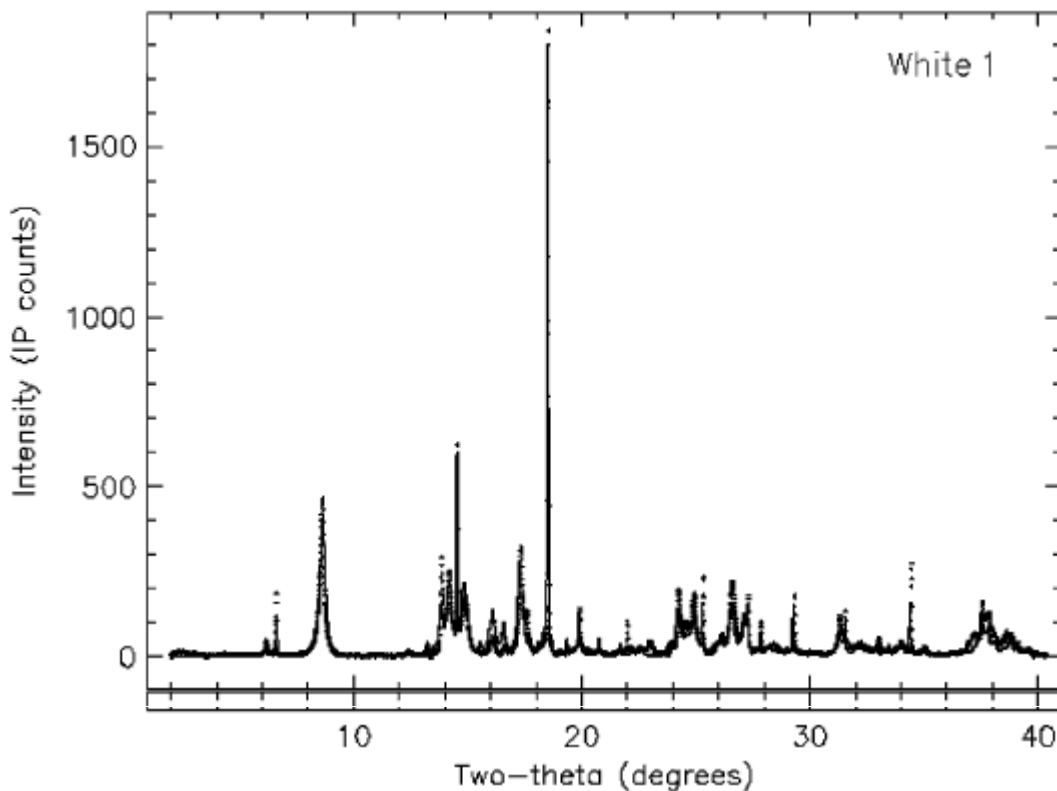


Fig. 4. Synchrotron radiation X-ray diffraction pattern from a white pigment used by indigenous artists of the Arnhem Land region.

Kulturní dědictví

The characterization of artefacts of cultural heritage
significance using physical techniques

Radiation Physics and Chemistry 74 (2005) 426–442

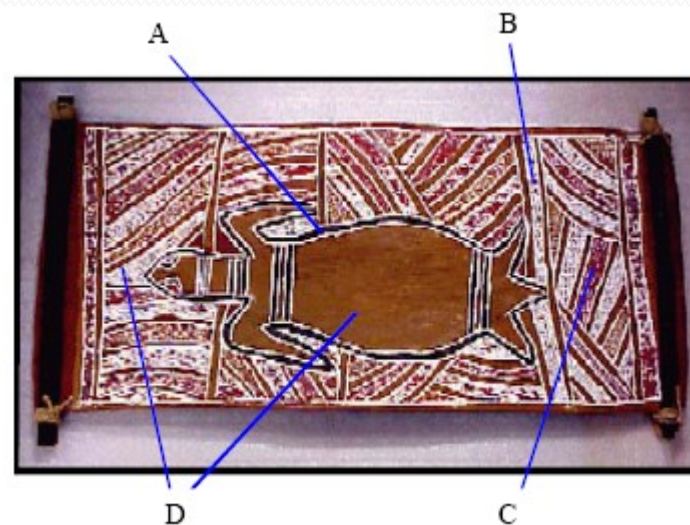
D.C. Creagh

Cultural Heritage Research Centre, Division of Science and Design, University of Canberra, Canberra ACT 2601, Australia

Table 2

Compositions of white pigments used by indigenous artists in
Arnhem Land

Sample	Mineral	% composition
1	Kaolinite	74
	Quartz	18
	Talc	2
	Muscovite	3
	Other	3
3	Talc	98
	Hydroxyapatite	2
	Other	
4	Hundtite	81
	Quartz	4
	Other	15
5	Talc	98
	Hydroxyapatite	2
	Other	



Kulturní dědictví

The characterization of artefacts of cultural heritage
significance using physical techniques

Radiation Physics and Chemistry 74 (2005) 426–442

D.C. Creagh

Cultural Heritage Research Centre, Division of Science and Design, University of Canberra, Canberra ACT 2601, Australia



Fig. 8. Joe Byrne's armour.

Table 3

Percentage compositions of principal atomic compositions of the steel components of Joe Byrne's armour

Item		Mn	Fe	As	Sn	W	Pb
HELMET	Faceplate	0.32	96.56	0.17	1.80		0.18
HELMET	Cylinder		94.6	0.1	2.6		0.18
BREASTPLATE	General	0.33	96.85	0.07	1.48		0.14
BREASTPLATE	Mark, front	0.27	75.35	3.15	1.14	3.17	14.4
BREASTPLATE	Mark, back	0.48	97.88		0.48		0.20
BACKPLATE	General	0.32	96.56	0.17	1.80		0.18
LAP PLATE	General	0.31	94.29	0.10	2.6		0.18
SIDE PANEL 1	General		95.33	0.11	2.6		0.18
SIDE PANEL 2	General		98.14	0.25	0.47		0.09
RIVET	Typical		97.65		1.34		
MILD STEEL	Kandra	0.44	98.6				
MILD STEEL	Modern	1.07	94.57		2.15		

General means that the measurements have been made at a number of points on the item. Those items with a manganese composition came from material made after 1856. Note the significant difference in the apparent composition between measurements made on the mark on the breastplate and that made at the back, behind the mark. This is due to the absorption of the FeK α fluorescent radiation by the lead and tungsten.

Kulturní dědictví



Characterization of iron oxide-based pigments by synchrotron-based micro X-ray diffraction

L.K. Herrera ^{a,*}, M. Cotte ^{b,c}, M.C. Jimenez de Haro ^a, A. Duran ^a, A. Justo ^a, J.L. Perez-Rodriguez ^a

^a Materials Science Institute of Seville, CSIC, Avda. Americo Vesputio, 41092-Seville, Spain

^b European Synchrotron Radiation Facility, BP 220, 38043 Grenoble Cedex, France

^c Centre de Recherche et de Restauration des Musées de France (C2RMF), CNRS UMR 171, Palais du Louvre, Porte des Lions, 14, quai François Mitterrand, 75001 Paris, France

Applied Clay Science 42 (2008) 57–62

The characterization of iron in microsamples by conventional X-ray diffraction is difficult due to its low concentration in thin layers and its low reflecting power relative to other phases. Synchrotron radiation can provide unique information because of high intensity, sample penetration, small beam diameter and fast data collection. In this study, micro X-ray diffraction (μ -XRD) data were obtained of two samples taken from wall paintings at San Agustin's Church in Cordoba. Crystalline iron phases such as goethite, lepidocrocite and hematite in the cross-section of the painting thin layers were identified, with a good spatial resolution. Conventional XRD only detected hydrocerussite and cerussite rather than the full range of iron phases found in the μ -XRD experiments.

The same cross-section is appropriated for the application of other analytical techniques, such as energy dispersive X-ray spectroscopy, micro-Raman, and micro-FTIR spectroscopy. Analyses carried out using these techniques allow identification of pigments, supports and binders with the removal of just one sample, thereby significantly reducing damage to the artwork (Flieder, 1968; Van't Hul-Ehrnreich, 1970; Rimaldi, 1994; Brieni et al., 1999). These techniques also provide important information about the chemical composition of the ochre pigments used in the paints. However, it is not possible to characterize the different crystalline phases present.



Fig. 1. Photograph of a wall painting at San Agustin's Church in Cordoba, Spain.

Kulturní dědictví



Characterization of iron oxide-based pigments by synchrotron-based micro X-ray diffraction

L.K. Herrera ^{a,*}, M. Cotte ^{b,c}, M.C. Jimenez de Haro ^a, A. Duran ^a, A. Justo ^a, J.L. Perez-Rodriguez ^a

^a Materials Science Institute of Seville, CSIC, Avda. Americo Vesputio, 41092-Seville, Spain

^b European Synchrotron Radiation Facility, BP 220, 38043 Grenoble Cedex, France

^c Centre de Recherche et de Restauration des Musées de France (C2RMF), CNRS UMR 171, Palais du Louvre, Porte des Lions, 14, quai François Mitterrand, 75001 Paris, France

Applied Clay Science 42 (2008) 57–62

The use of synchrotron radiation (SR) sources by materials scientists for Cultural Heritage studies is comparatively new. The principal properties of synchrotron radiation are as follows: High flux of the source and brilliance allow fast data acquisition, with a good signal-to-noise ratio, and the small beam footprint allows 2D and 3D studies to be performed on the submillimeter/micrometer length scale, thereby allowing use of small samples. The broad spectral output of synchrotron sources also provides for wavelength tunability, thereby allowing selection of the energy region most suitable for a given problem (Cotte et al., 2007).

Kulturní dědictví



Characterization of iron oxide-based pigments by synchrotron-based micro X-ray diffraction

L.K. Herrera ^{a,*}, M. Cotte ^{b,c}, M.C. Jimenez de Haro ^a, A. Duran ^a, A. Justo ^a, J.L. Perez-Rodriguez ^a

^a Materials Science Institute of Seville, CSIC, Avda. Americo Vesputio, 41092-Seville, Spain

^b European Synchrotron Radiation Facility, BP 220, 38043 Grenoble Cedex, France

^c Centre de Recherche et de Restauration des Musées de France (C2RMF), CNRS UMR 171, Palais du Louvre, Porte des Lions, 14, quai François Mitterrand, 75001 Paris, France

Applied Clay Science 42 (2008) 57–62

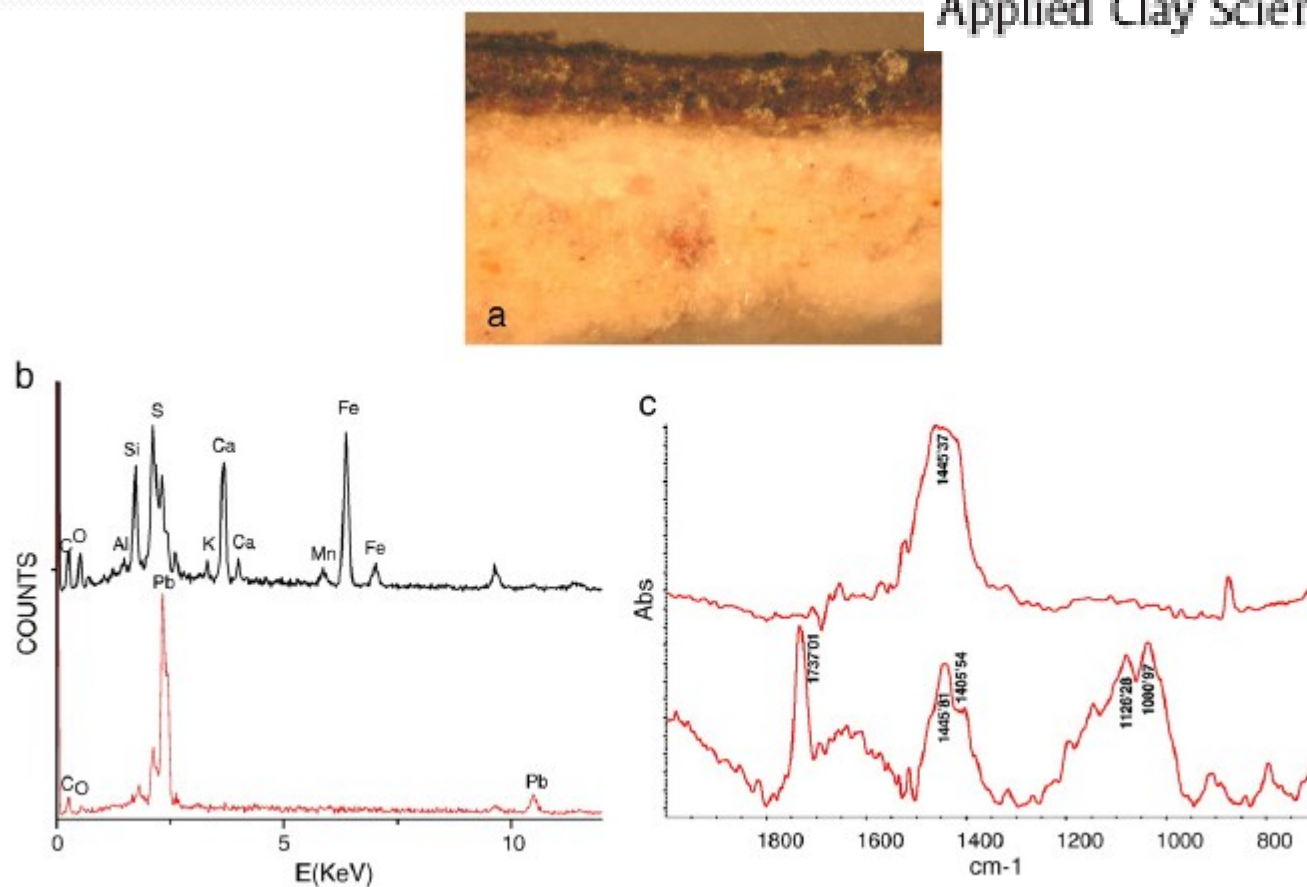


Fig. 3. (a) Cross-sections of sample 1 (b) EDX analysis of two layers (c) FTIR of the two layers. (For interpretation of the references to color in this figure legend, the reader is referred to the web version of this article.)

Kulturní dědictví



Characterization of iron oxide-based pigments by synchrotron-based micro X-ray diffraction

L.K. Herrera ^{a,*}, M. Cotte ^{b,c}, M.C. Jimenez de Haro ^a, A. Duran ^a, A. Justo ^a, J.L. Perez-Rodriguez ^a

^a Materials Science Institute of Seville, CSIC, Avda. Americo Vesputio, 41092-Seville, Spain

^b European Synchrotron Radiation Facility, BP 220, 38043 Grenoble Cedex, France

^c Centre de Recherche et de Restauration des Musées de France (C2RMF), CNRS UMR 171, Palais du Louvre, Porte des Lions, 14, quai François Mitterrand, 75001 Paris, France

Applied Clay Science 42 (2008) 57–62

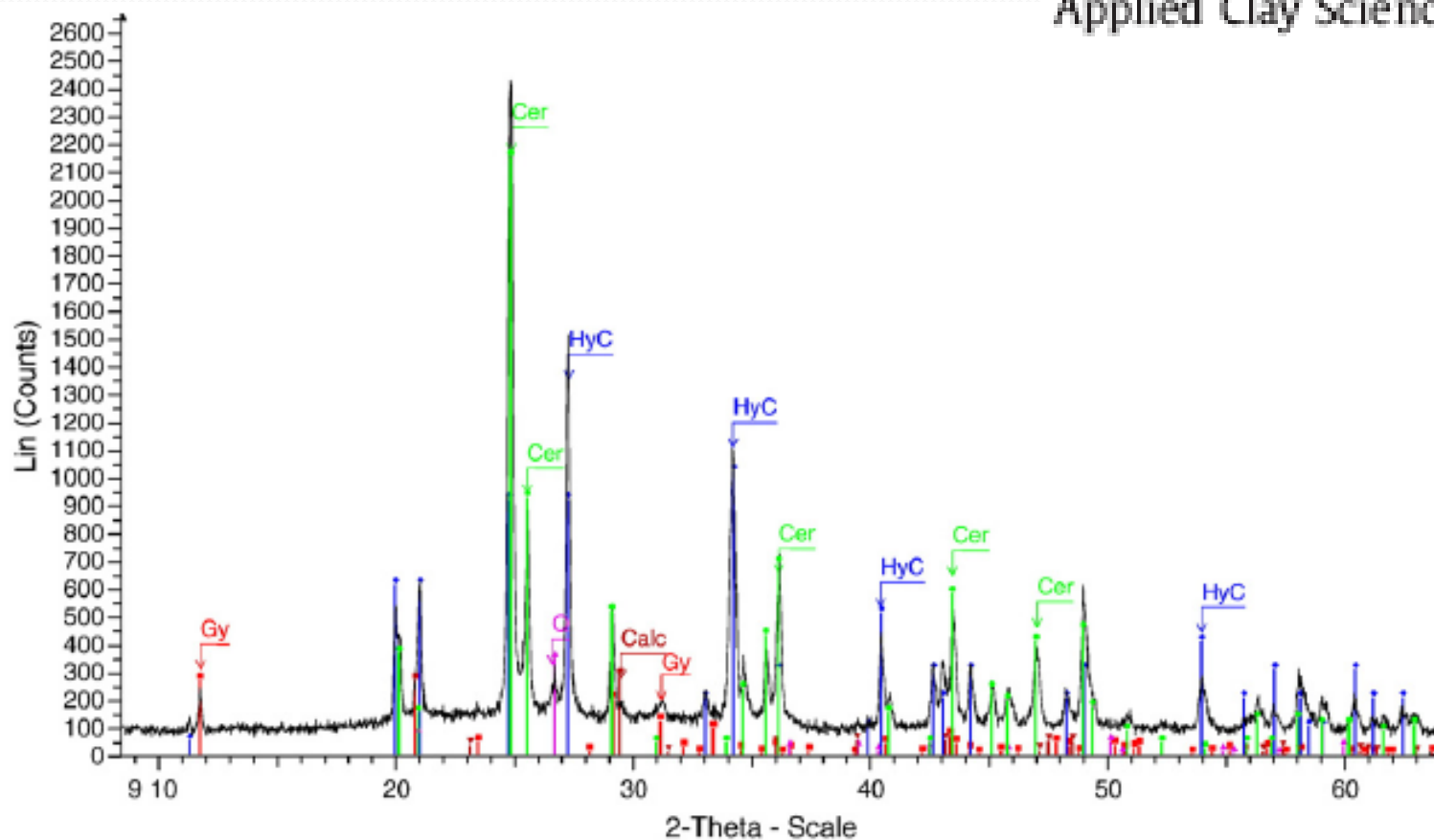


Fig. 5. The X-ray diffraction pattern of the powdered sample 1 obtained with conventional Bragg–Brentano geometry.

Kulturní dědictví



Characterization of iron oxide-based pigments by synchrotron-based micro X-ray diffraction

L.K. Herrera ^{a,*}, M. Cotte ^{b,c}, M.C. Jimenez de Haro ^a, A. Duran ^a, A. Justo ^a, J.L. Perez-Rodriguez ^a

^a Materials Science Institute of Seville, CSIC, Avda. Americo Vespucio, 41092-Seville, Spain

^b European Synchrotron Radiation Facility, BP 220, 38043 Grenoble Cedex, France

^c Centre de Recherche et de Restauration des Musées de France (C2RMF), CNRS UMR 171, Palais du Louvre, Porte des Lions, 14, quai François Mitterrand, 75001 Paris, France

Applied Clay Science 42 (2008) 57–62

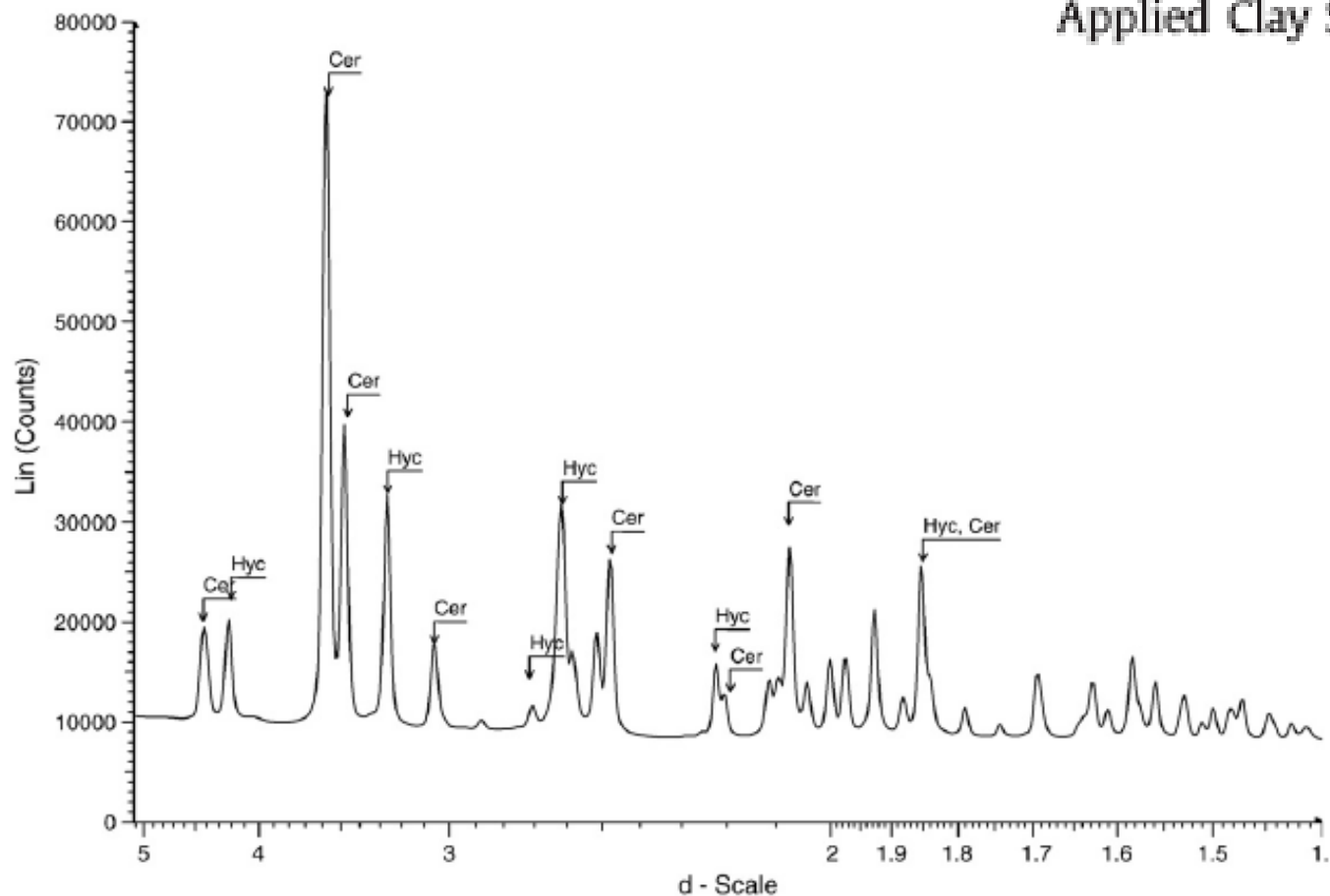


Fig. 8. μ -XRD pattern white layer of sample 1.

Kulturní dědictví



Characterization of iron oxide-based pigments by synchrotron-based micro X-ray diffraction

L.K. Herrera ^{a,*}, M. Cotte ^{b,c}, M.C. Jimenez de Haro ^a, A. Duran ^a, A. Justo ^a, J.L. Perez-Rodriguez ^a

^a Materials Science Institute of Seville, CSIC, Avda. Americo Vespucio, 41092-Seville, Spain

^b European Synchrotron Radiation Facility, BP 220, 38043 Grenoble Cedex, France

^c Centre de Recherche et de Restauration des Musées de France (C2RMF), CNRS UMR 171, Palais du Louvre, Porte des Lions, 14, quai François Mitterrand, 75001 Paris, France

Applied Clay Science 42 (2008) 57–62

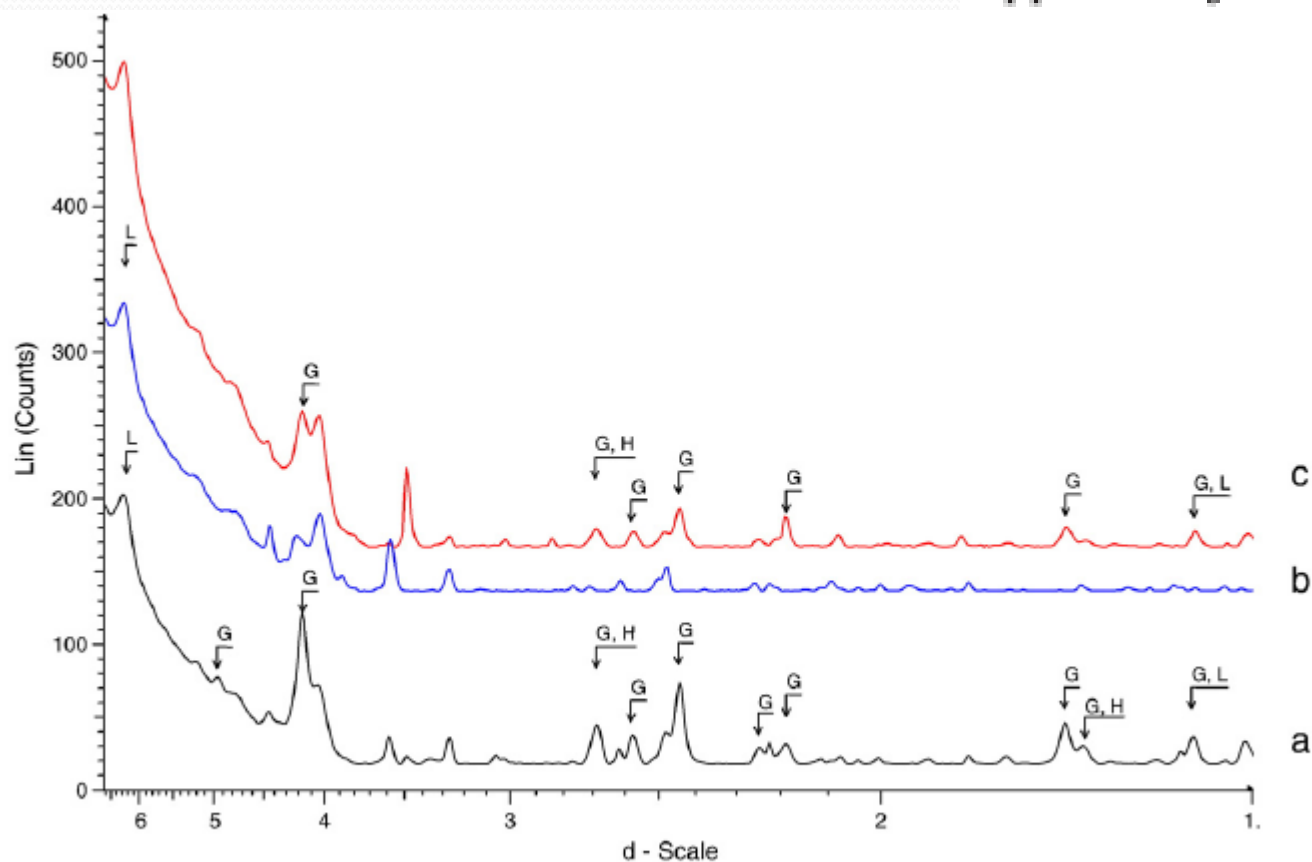


Fig. 9. μ -XRD patterns of dark brown layer of sample 1. (For interpretation of the references to color in this figure legend, the reader is referred to the web version of this article.)

Rentgenová difraktometrie monokrystal

Single-crystal X-ray Diffraction is a non-destructive analytical technique which provides detailed information about the internal lattice of crystalline substances, including unit cell dimensions, bond-lengths, bond-angles, and details of site-ordering.

Directly related is single-crystal refinement, where the data generated from the X-ray analysis is interpreted and refined to obtain the crystal structure.

Rentgenová difraktometrie

monokrystal

In an X-ray diffraction measurement, a crystal is mounted on a goniometer and gradually rotated while being bombarded with X-rays, producing a diffraction pattern of regularly spaced spots known as *reflections*.

The two-dimensional images taken at different rotations are converted into a three-dimensional model of the density of electrons within the crystal using the mathematical method of Fourier transforms, combined with chemical data known for the sample.

Poor resolution (fuzziness) or even errors may result if the crystals are too small, or not uniform enough in their internal makeup.

Rentgenová difraktometrie monokrystal

The crystal scatters the X-rays into a pattern of spots or reflections that can be observed on a screen behind the crystal. The relative intensities of these spots provide the information to determine the arrangement of molecules within the crystal in atomic detail.

The intensities of these reflections may be recorded with photographic film, an area detector or with a charge-coupled device (CCD) image sensor.

The peaks at small angles correspond to low-resolution data, whereas those at high angles represent high-resolution data; thus, an upper limit on the eventual resolution of the structure can be determined from the first few images.

Rentgenová difraktometrie monokrystal

- an X-ray source consisting of a high-stability X-ray generator, a copper or molybdenum target X-ray tube, a tube shield with associated shutters, attenuators and safety interlocks, a monochromator or X-ray mirror system, and an incident-beam collimator;
- a three- or four-circle goniometer system that allows the specimen to be precisely oriented in any position while remaining in the X-ray beam;
- a video camera or microscope for aligning the specimen and indexing crystal faces;
- a CCD-based two-dimensional X-ray detector system;
- a low-temperature attachment for cooling the specimen during data collection;
- a microprocessor-based interface module that receives commands from a host computer and carries out all real-time instrument control functions to drive goniometer motors, monitor the detector system, open and close the shutter and monitor collision sensors and safety interlocks;

Rentgenová difraktometrie monokrystal

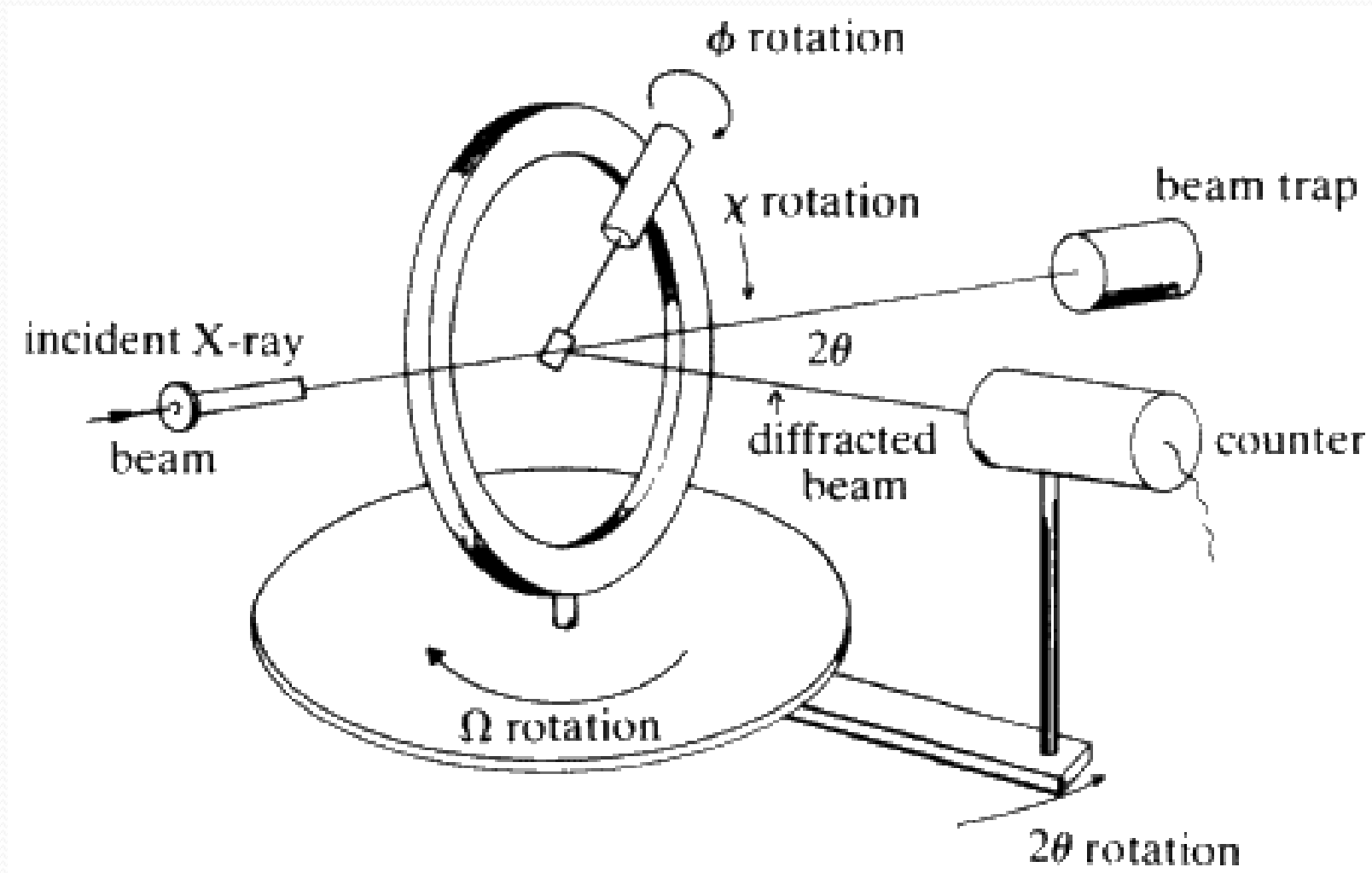
The mounted crystal is irradiated with a beam of monochromatic X-rays.

The brightest and most useful X-ray sources are synchrotrons; their much higher luminosity allows for better resolution.

They also make it convenient to tune the wavelength of the radiation.

Synchrotrons are generally national facilities, each with several dedicated beamlines where data is collected around the clock, seven days a week.

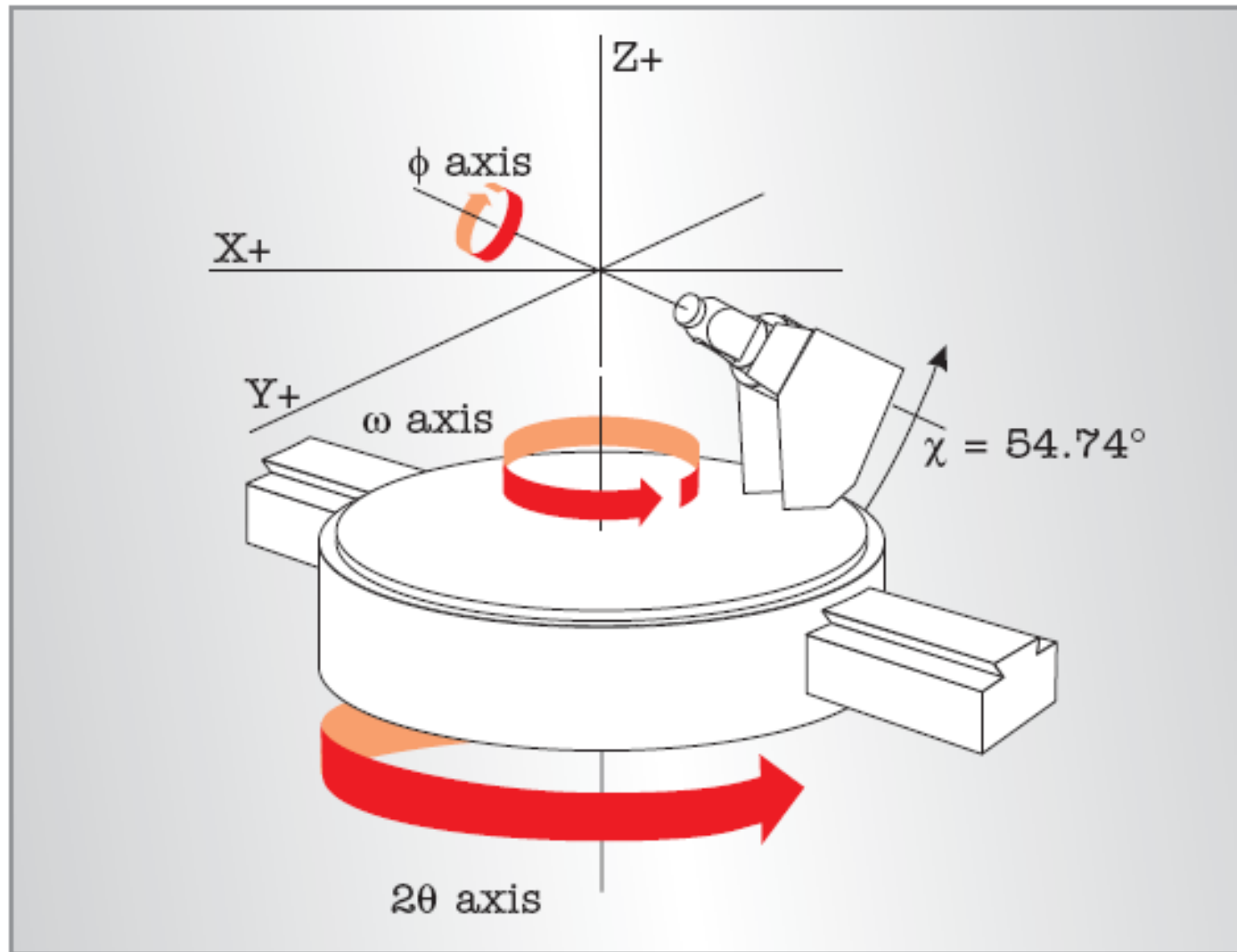
Rentgenová difraktometrie monokrystal



Rentgenová difraktometrie monokrystal



Rentgenová difraktometrie monokrystal



Rentgenová difraktometrie monokrystal

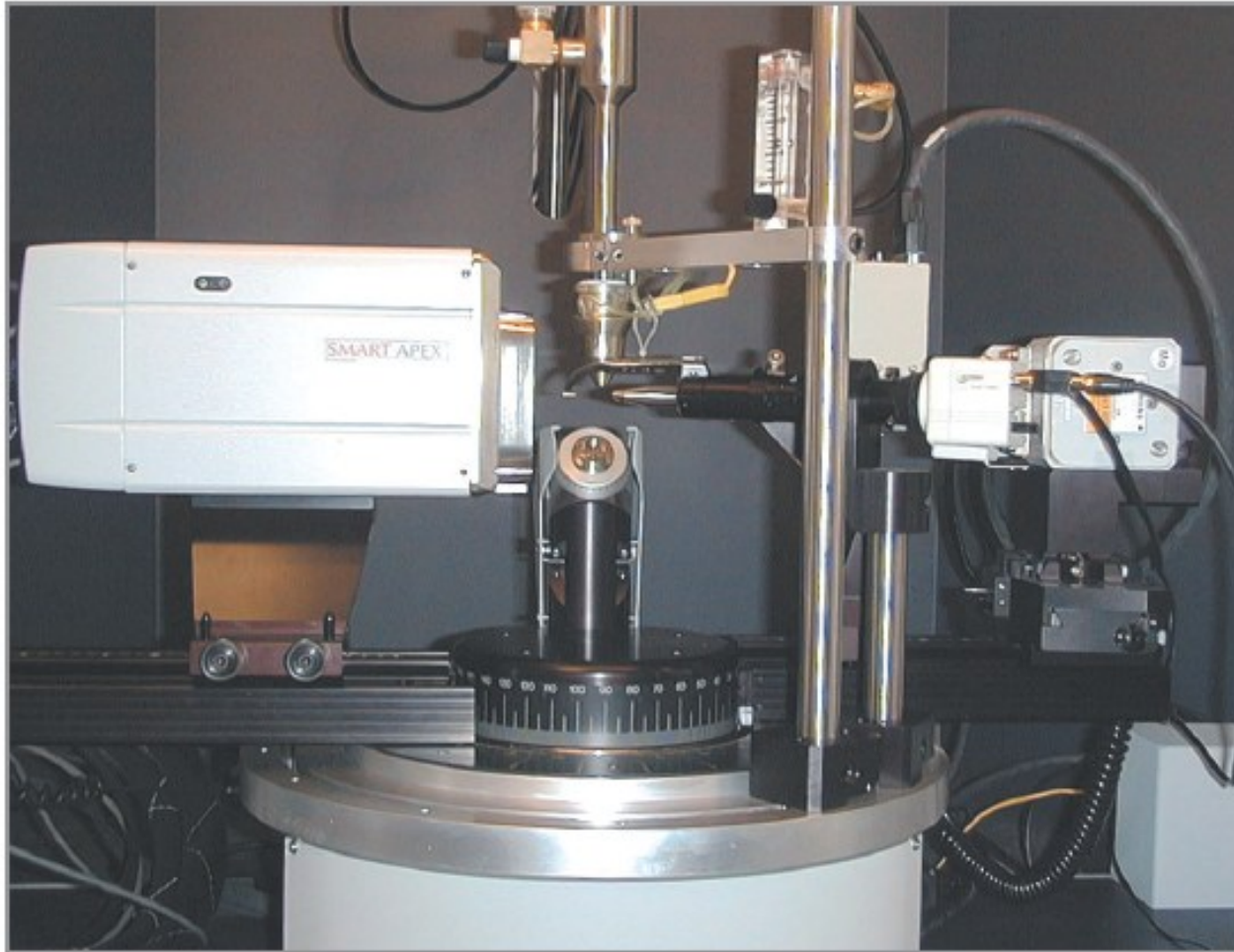


Figure 7. A commercial CCD-based single-crystal X-ray diffractometer system (courtesy of Bruker AXS Inc.)

Rentgenová difraktometrie monokrystal

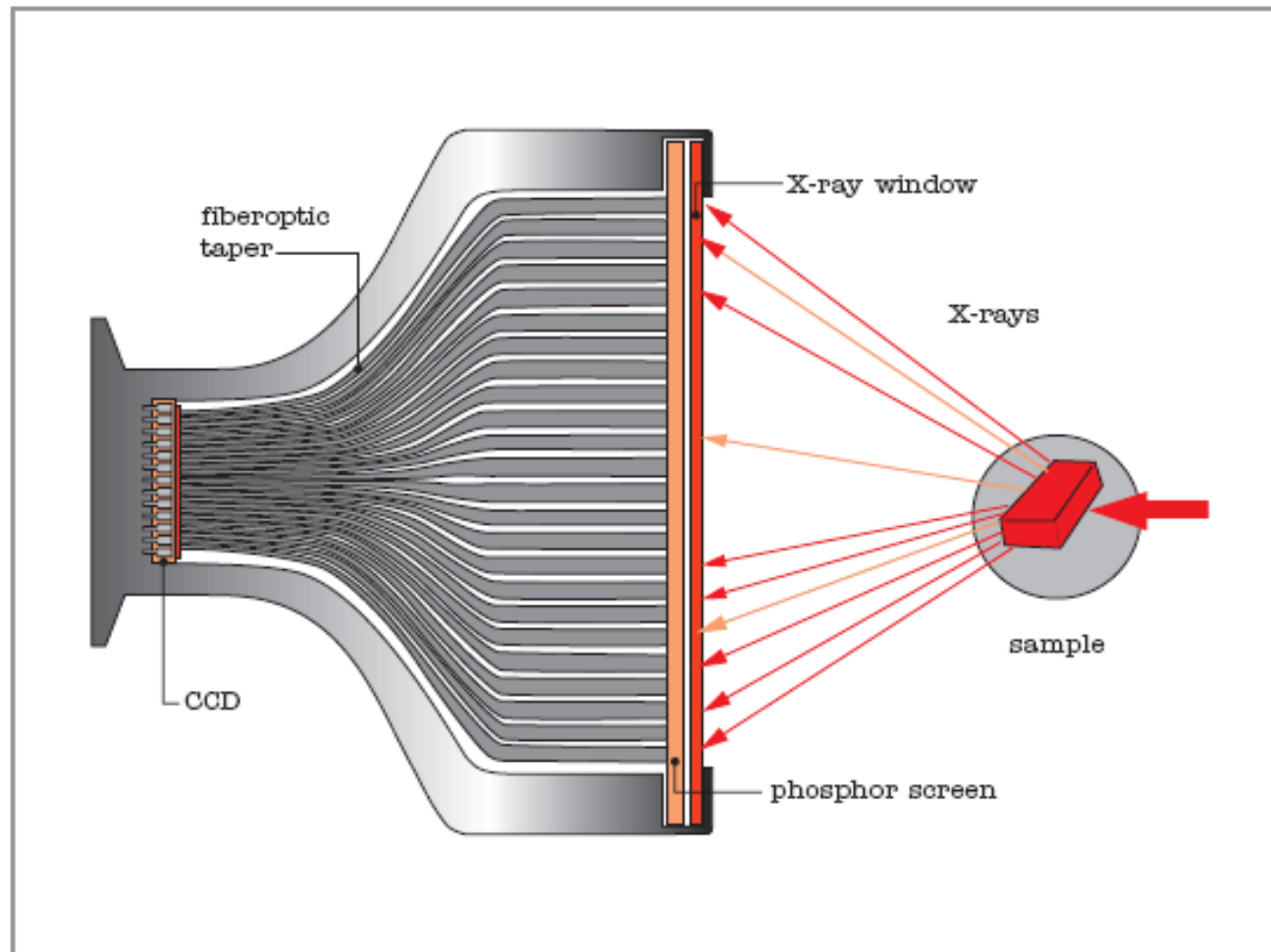


Figure 8. Diagram of a typical CCD detector used for X-ray diffraction.

Rentgenová difraktometrie monokrystal

The first atomic-resolution structure to be "solved" (i.e. determined) in 1914 was that of **table salt**. **The distribution of electrons** in the table-salt structure showed that crystals are not necessarily composed of **covalently bonded** molecules, and proved the existence of **ionic compounds**.

The structure of **diamond** was solved in the same year, proving the tetrahedral arrangement of its chemical bonds and showing that the length of C-C single bond was 1.52 Ångströms.

Other early structures included **copper**, **calcium fluoride** (*fluorite*), **calcite** (CaCO_3) and **pyrite** (FeS_2) in 1914; **spinel** (MgAl_2O_4) in 1915; the **rutile** and **anatase** forms of **titanium dioxide** in 1916; **pyrochroite** $\text{Mn}(\text{OH})_2$ and **brucite** $\text{Mg}(\text{OH})_2$ in 1919; and **wurtzite** (hexagonal ZnS) in 1920.

Rentgenová difraktometrie monokrystal

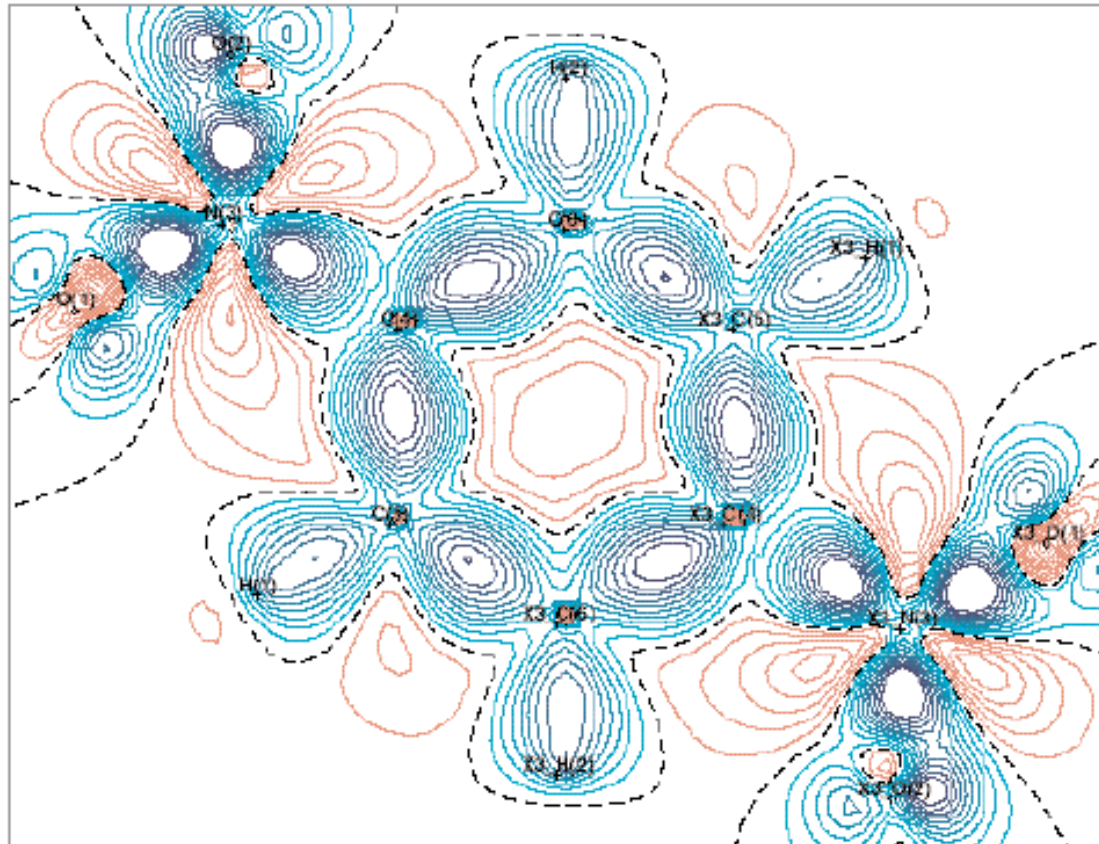
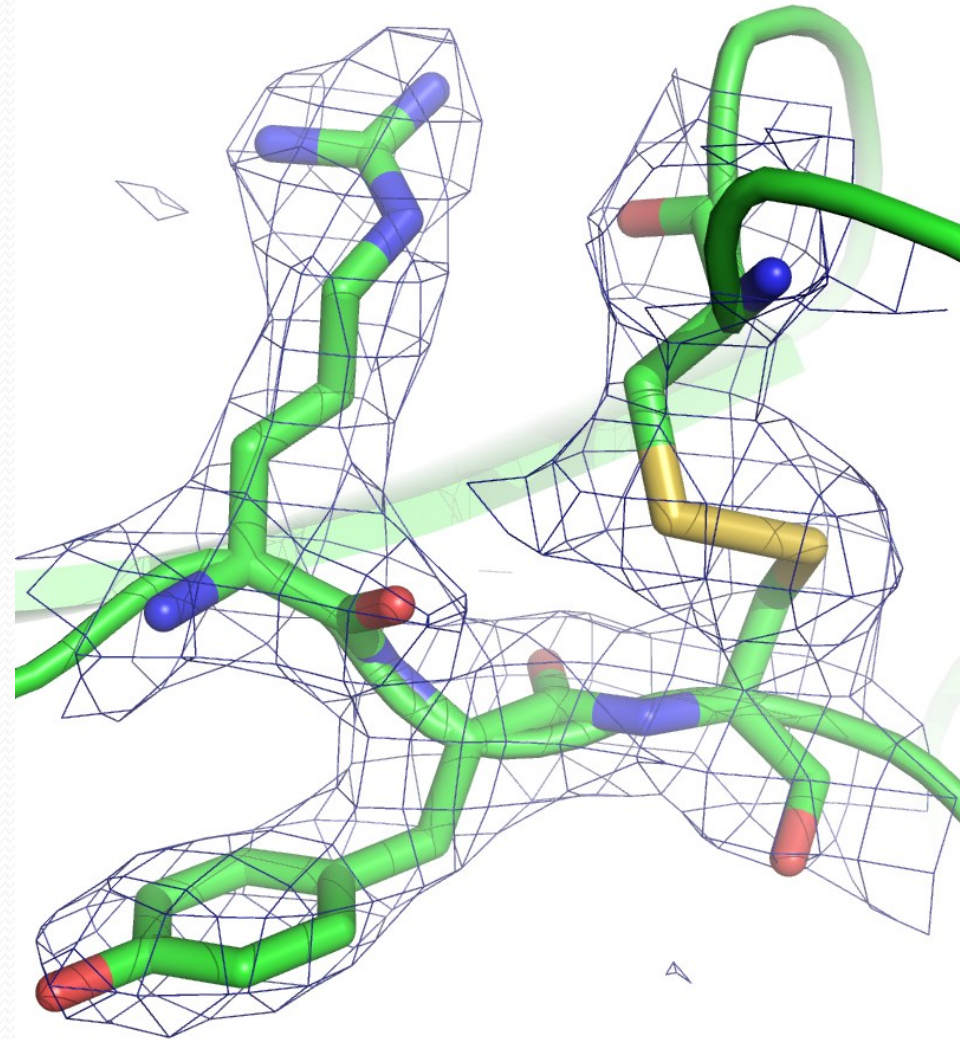
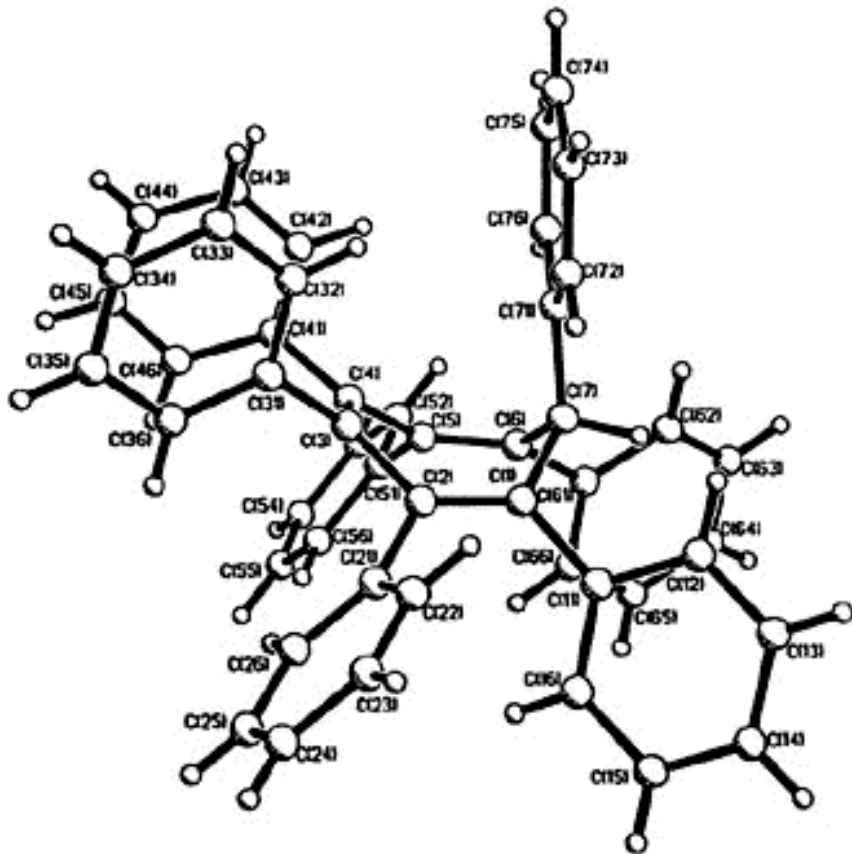


Figure 1. Electron density difference map for p-dinitrobenzene obtained by subtracting the promolecule electron density from the total electron density.

Rentgenová difraktometrie monokrystal



Rentgenová difraktometrie monokrystal

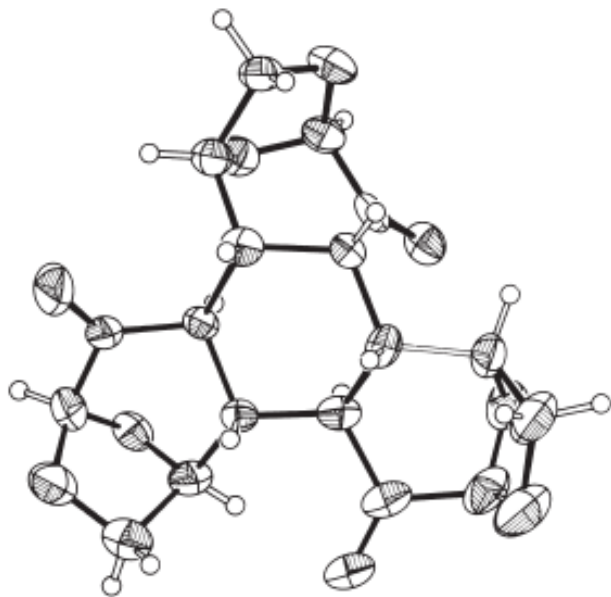


Figure 9. Thermal ellipsoid plot of the final structure of an organic compound (C₁₈H₁₈O₉).

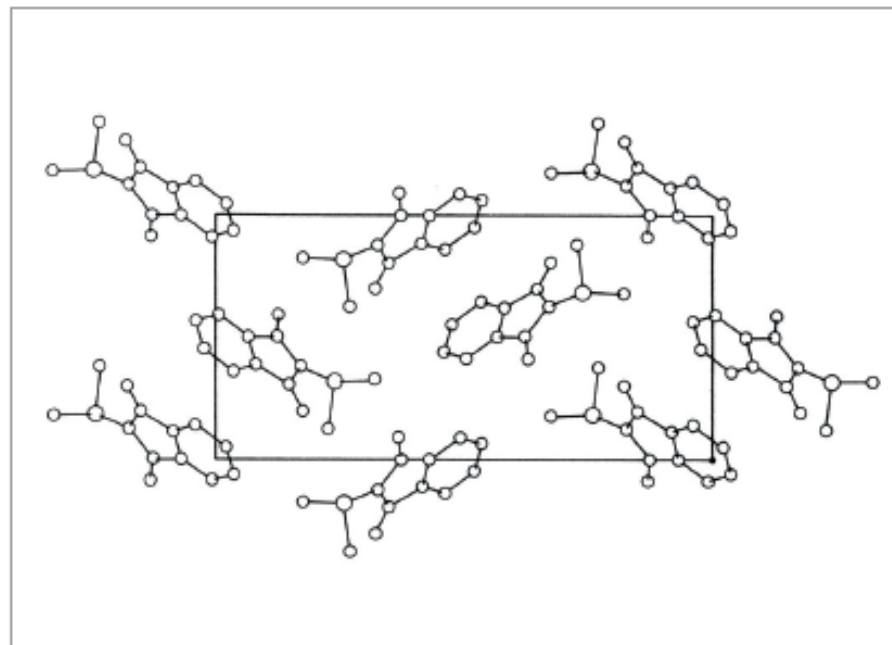


Figure 10. Unit-cell diagram showing the arrangement of molecules within the cell.

Rentgenová difraktometrie monokrystal

